

Figure S6.

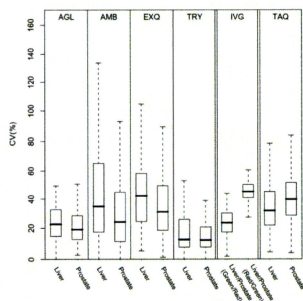
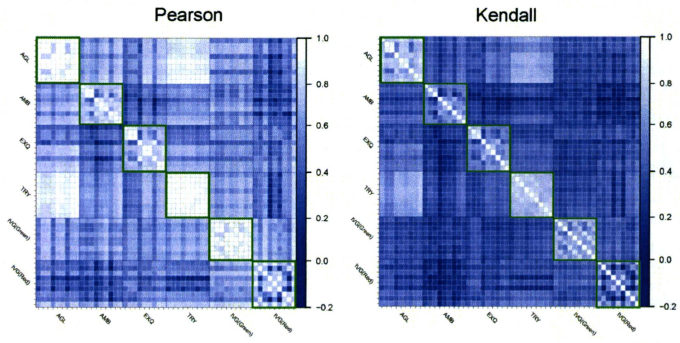


Figure S7.



MicroRNA-210 Regulates Cancer Cell Proliferation through Targeting Fibroblast Growth Factor Receptor-like 1 (FGFRL1)[†]

Received for publication, July 30, 2010, and in revised form, October 29, 2010. Published, JBC Papers in Press, November 2, 2010, DOI 10.1074/jbc.M110.170852

Soken Tsuchiya[‡], Takeshi Fujiwara[‡], Fumiaki Sato[‡], Yutaka Shimada[§], Eiji Tanaka[¶], Yoshiharu Sakai[¶], Kazuharu Shimizu[‡], and Gozoh Tsujimoto^{¶1}

From the [‡]Department of Nanobio Drug Discovery, Graduate School of Pharmaceutical Sciences, Kyoto University, 46-29 Yoshida Shimoadachi, Sakyo-ku, Kyoto 606-8501, Japan, the [§]Department of Surgery and Science, Graduate School of Medicine and Pharmaceutical Sciences for Research, University of Toyama, 2630 Sugitani, Toyama 930-0194, Japan, the [¶]Department of Surgery, Graduate School of Medicine, Kyoto University, 54 Shogoin Kawara-cho, Sakyo-ku, Kyoto 606-8507, Japan, and the [†]Department of Genomic Drug Discovery Science, Graduate School of Pharmaceutical Sciences, Kyoto University, 46-29 Yoshida Shimoadachi, Sakyo-ku, Kyoto 606-8501, Japan

The importance of microRNAs (miRNAs) in human malignancies has been well recognized. Here, we report that the expression of microRNA-210 (miR-210) is down-regulated in human esophageal squamous cell carcinoma and derived cell lines. Marked decreases in the level of miR-210 were observed especially in poorly differentiated carcinomas. We found that miR-210 inhibits cancer cell survival and proliferation by inducing cell death and cell cycle arrest in G₁/G₀ and G₂/M. Finally, we identified fibroblast growth factor receptor-like 1 (FGFRL1) as a target of miR-210 in esophageal squamous cell carcinoma and demonstrated that FGFRL1 accelerates cancer cell proliferation by preventing cell cycle arrest in G₁/G₀. Taken together, our findings show an important role for miR-210 as a tumor-suppressive microRNA with effects on cancer cell proliferation.

MicroRNAs (miRNAs)² are evolutionarily conserved small noncoding RNAs (20–23 nucleotides) that bind to complementary sequences in the 3'-untranslated region (UTR) of target messenger RNAs (mRNAs) and regulate gene expression by the cleavage of target mRNAs and/or translational inhibition (1). Currently, >800 human miRNAs have been identified and registered in the miRNA database, miRBase (2). miRNAs play important roles in the differentiation of various cell types and in the initiation and progression of cancer, and it has been shown that the expression of some miRNAs is altered during cell differentiation and in malignancies (1, 3, 4).

In a recent study, we identified microRNA-210 (miR-210) as one of the miRNAs that is markedly differentially expressed during the process of epithelial differentiation (3). It has been reported that miR-210 expression is down-regulated during epithelial-mesenchymal transition, the aberrant activation of which triggers cancer pathology (5). Carcinomas are derived from epithelial cells, and poor prognosis in patients with carcinoma is associated with the disruption of characteristics of differentiated epithelial cells, such as cell junctions and polarity (6–8). Hence, given that the expression of miR-210 appears to be correlated well with epithelial differentiation, miR-210 might play a suppressive role in carcinomas. In support of this idea, allelic deletions at the miR-210 locus have been observed in 64% of cases of ovarian cancer (9), and ectopic expression of miR-210 represses tumor growth when human cancer cell lines are implanted into immunodeficient mice (10). However, the clinical roles of miR-210 in carcinomas and the mechanisms by which it represses tumor growth remain unknown.

In this study, we investigated the functional role of miR-210 in the growth of carcinomas and the mechanism by which it acts using clinical samples as well as cell lines of esophageal squamous cell carcinoma (ESCC). ESCC is a highly aggressive malignancy with a 5-year survival rate of 10% worldwide. It has been used as a model to study the mechanisms of dysregulated epithelial differentiation and epithelial-mesenchymal transition in carcinomas (11, 12).

EXPERIMENTAL PROCEDURES

Specimens—All tumor samples were confirmed as ESCC by the Clinicopathologic Department at Kyoto University Hospital. All cases were classified according to the sixth edition of the pathologic tumor-node-metastasis (TNM) classification (13). Written informed consent for the research use was obtained from each patient before surgery. The study was approved by the Kyoto University Institutional Review Board.

Cell Culture and Transfection—HE3 cells, which are human primary normal esophageal epithelial cells, were established and cultured in keratinocyte SFM (Invitrogen) containing human recombinant epidermal growth factor (Invitrogen) and bovine pituitary extract (Invitrogen). HEEpiC cells were purchased from ScienCell Research Laboratories (Carlsbad,

* This work was supported by grants from Kyoto University (to S. T.), the Takeda Science Foundation (to S. T.), the Ministry of Education, Culture, Sports, Science and Technology of Japan (to S. T. and G. T.), and the New Energy and Industrial Technology Development Organization (to G. T.).

[†] The on-line version of this article (available at <http://www.jbc.org>) contains supplemental Tables 1–3.

The data reported in this paper have been deposited in the Gene Expression Omnibus (GEO) database, www.ncbi.nlm.nih.gov/geo (accession no. GSE20637).

¹ To whom correspondence should be addressed. Tel.: 81-75-753-4523; Fax: 81-75-753-4544; E-mail: gtsuji@pharm.kyoto-u.ac.jp.

² The abbreviations used are: miRNA, microRNA; ESCC, esophageal squamous cell carcinoma; FGFRL1, fibroblast growth factor receptor-like 1; miR-210, microRNA-210; ncRNA, negative control RNA; ncsiRNA, negative control small interfering RNA; NEST, normal esophageal squamous tissue; PI, propidium iodide; qRT-PCR, quantitative reverse transcriptase-PCR.

CA) and were cultured according to the manufacturer's instructions (14). The human ESCC cell lines KYSE-150, -170, -190, and -590 were maintained as described previously (14, 15). KYSE-170 cells were transfected with oligoribonucleotides for miR-210 or negative control RNA (ncRNA) (Ambion, Austin, TX) using HiPerFect transfection reagent (Qiagen, Valencia, CA) according to the manufacturer's protocol for overexpression. KYSE-170 cells were also transfected with *FGFR1* (fibroblast growth factor receptor-like 1) small interfering RNAs (siRNAs) or negative control siRNA (ncsiRNA) (Invitrogen) for knockdown of *FGFR1*. The coding region of *FGFR1* was isolated from complementary DNA (cDNA) from KTSE-170 cells, which was reverse transcribed using an oligo(dT) primer (Invitrogen), and ligated into the pcDNA3 expression vector. This *FGFR1* expression construct was transfected into KYSE-170 cells using TransIT-LT1 transfection reagent (Mirus, Madison, WI). For inhibition of miRNAs function, KYSE-590 cells were transfected with a specific microRNA inhibitor for miR-210 (anti-miR-210) or its negative control RNA (anti-ncRNA) (Ambion) using HiPerFect transfection reagent.

RNA Extraction and Quantitative Reverse Transcriptase-PCR—Total RNA was extracted from the normal esophageal squamous tissues (NESTs), ESCCs, and cell lines by the acid guanidinium thiocyanate-phenol-chloroform method and then used for quantitative reverse transcriptase-PCR (qRT-PCR). To quantify mRNA expression levels, total RNA was reverse transcribed to cDNA using random primers and SuperScript II reverse transcriptase (Invitrogen), and quantitative PCR was performed in a 7300 Real-Time PCR System (Applied Biosystems) using Power SYBR Green PCR Master Mix (Applied Biosystems). Gene expression was quantified using standard curves that were generated using serially diluted reference samples and normalized to the expression level of glyceraldehyde-3-phosphate dehydrogenase (*GAPDH*). The specificity of the PCR products was confirmed by gel electrophoresis and a dissociation curve analysis. Primer sequences are shown in supplemental Table 1. To quantify the levels of miRNAs and RNA U6 small nuclear 2 (*RNU6-2*), we used TaqMan MicroRNA assays (Applied Biosystems), which detect mature miRNAs specifically, following the manufacturer's protocol. The miRNA expression level was normalized to the expression level of *RNU6-2*.

Assay of Cell Proliferation, Cell Cycle, and Cell Death—The WST-1 assay to measure cell proliferation and flow cytometric assays to analyze the cell cycle and cell death were performed with KYSE-170 cells at 48 h after transfection as described previously (15). Calculations for the analysis of the cell cycle were performed with ModFit software (BD Biosciences). The bromodeoxyuridine (BrdU) incorporation assay, which measures cell proliferation, was performed using the BrdU Cell Proliferation ELISA kit (Roche Applied Science) according to the manufacturer's instructions.

Microarray Analysis—Total RNA from KYSE-170 cells that had been transfected with either ncRNA or miR-210 was labeled and prepared for hybridization to a human Oligo chip 25k (Toray, Tokyo, Japan) using standard methods. The GEO

database accession code of the microarray data obtained is GSE20637.

Immunoblot Analyses—Cells were homogenized and centrifuged. The resultant supernatant was subjected to SDS-PAGE, and the separated proteins were transferred electrophoretically onto a PVDF membrane. An anti-FGFR1, NDUFA4, GPR177, or LRP5L antibody (Santa Cruz Biotechnology, Santa Cruz, CA) (1:100) was used as the primary antibody, respectively, and a horseradish peroxidase-conjugated IgG antibody (1:5,000) was used as the secondary antibody. The membranes were stained using an ECL kit according to the manufacturer's instructions. An anti- β -actin antibody (Sigma-Aldrich) (1:1,000) was used as a control.

Immunostaining—Sections of ESCC and NEST were stained with an anti-FGFR1 antibody (Santa Cruz Biotechnology) and ChemMate ENVISION kit (Dako, Glostrup, Denmark).

Luciferase Reporter Assay—The 3'-UTRs of *FGFR1*, *WSB2*, and *GDI2* were isolated from cDNA from KTSE-170 cells. These 3'-UTRs and synthetic oligonucleotides of putative miR-210-target sites in the *FGFR1* 3'-UTR ligated into the pGL3 basic luciferase expression (pGL3-Luc) vector (Promega, Madison, WI) at the 3'-end of the luciferase coding sequence (Luc), respectively. This pGL3-Luc vector containing 3'-UTR or miR-210 target sites and the pRL-TK internal control vector (Promega) were transfected into KYSE-170 cells using FuGENE HD transfection reagent (Roche Applied Science). Oligoribonucleotides for miR-210 or ncRNA were transfected 24 h after transfection of their vectors, and luciferase activity was measured 38 h after transfection of their vectors using the Dual Luciferase Reporter Assay system (Promega) according to the manufacturer's instructions.

Statistics—Results are expressed as the mean \pm S.E. Student's *t* test was used to compare data between two groups. *p* values less than 0.05 were considered to be statistically significant. In Figs. 1C and 4E, each clinicopathologic parameter, with the exception of age, was evaluated using Pearson's χ^2 test.

RESULTS

MiR-210 Expression Is Significantly Down-regulated in ESCC, Especially in Poorly Differentiated Carcinomas—To investigate the role of miR-210 in human malignancies, we first examined the expression levels of miR-210 in clinical samples of matched NEST and ESCC by qRT-PCR (Fig. 1A). Compared with NEST, a significant down-regulation of miR-210 expression was noted in ESCC. On the other hand, the expression of miR-31, which has been reported to be not altered between ESCC and NEST (16, 17), showed no significant difference (Fig. 1B). For further analysis, 82 clinical samples of ESCC were divided into two groups (miR-210-high and miR-210-low) on the basis of their miR-210 expression levels, and the clinicopathologic characteristics of these two groups were assessed. A significant difference was observed between the miR-210-high group and the miR-210-low group with respect to histological type (*i.e.* well, moderately, and poorly differentiated), but there were no significant differences between the two groups with respect to gender, age, or

MicroRNA-210 Regulates Cancer Cell Cycle and Death

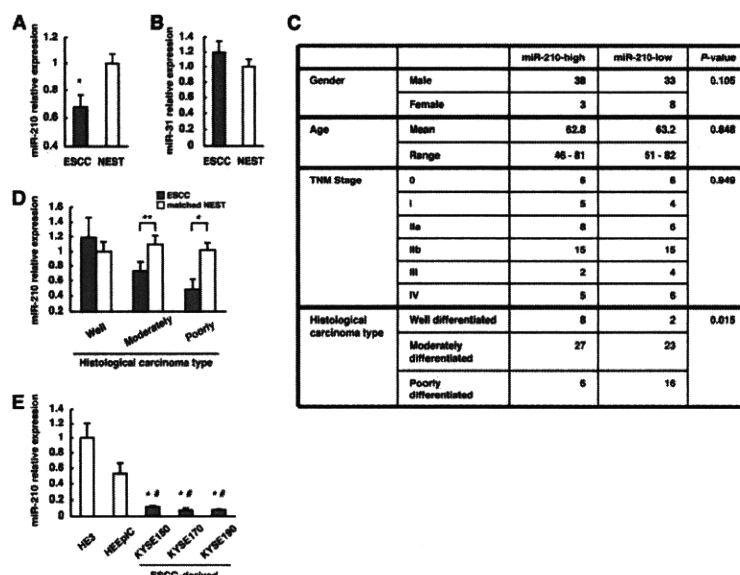


FIGURE 1. Down-regulation of miR-210 expression in ESCC. A and B, expression levels of miR-210 and miR-31 in NEST and ESCC assessed by qRT-PCR. The values are shown relative to the value obtained for NEST ($n = 82$; $p < 0.01$). C, clinicopathologic characteristics of 82 ESCCs divided into two groups ($n = 41$) on the basis of miR-210 expression levels. D, expression levels of miR-210 in the ESCCs and the corresponding NESTs in each histological type were compared by qRT-PCR. The values are shown relative to the value obtained for NEST in the well differentiated group (**, $p < 0.05$; *, $p < 0.01$). E, levels of miR-210 in HE3, HEEpiC, and KYSE cell lines analyzed by qRT-PCR. The values are shown relative to the value obtained for HE3 ($n = 3$; *, $p < 0.05$ versus HE3; #, $p < 0.05$ versus HEEpiC). Error bars, S.E.

pathologic TNM stage (Fig. 1C). Then, we compared the expression levels of miR-210 between ESCC and the matched NEST for each histological type. Significant differences were observed between moderately and poorly differentiated ESCC and the matched NEST (Fig. 1D). Moreover, as the degree of tumor differentiation decreased, the level of miR-210 showed a corresponding decrease in the ESCC ($p = 0.0875$, ANOVA) but not in the matched NEST ($p = 0.8728$, ANOVA), which indicated a strong correlation between the level of miR-210 and the degree of tumor differentiation in ESCC. This observation appears to agree well with the previous finding that miR-210 expression is up-regulated in parallel with epithelial cell differentiation (3, 18). Furthermore, when we compared the levels of miR-210 expression in normal human esophageal epithelial cells (HE3 and HEEpiC) with those in ESCC cell lines (KYSE-150, -170, and -190), we found that miR-210 expression was down-regulated significantly in the ESCC cell lines (Fig. 1E).

miR-210 Inhibits Cancer Cell Proliferation by Inducing Cell Death and Cell Cycle Arrest in G_1/G_0 and G_2/M —Next, we examined the functional role of miR-210 in ESCC by adding synthetic miR-210 to the KYSE-170 cell line, in which miR-210 expression is low (Fig. 1E). Given that miR-210 expression was correlated with the level of differentiation in ESCC (Fig. 1, C and D), we examined the effect of miR-210 on the proliferation of ESCC cells. Transfection of miR-210 significantly decreased the proliferation of cancer cells, whereas a ncRNA had no inhibitory effect (Fig. 2A). Then, the introduced amount of miR-210 in cells transfected with miR-210

was a >60-fold increase compared with ones in cells transfected with ncRNA (Fig. 2B), which is within the comparable range for the differences between normal human esophageal epithelial cells and KYSE-170 cells (Fig. 1E). Moreover, we performed a BrdU incorporation assay and found that miR-210 significantly reduced the uptake of BrdU (Fig. 2C). These results suggested that miR-210 negatively regulates cancer cell proliferation. Next, we examined the effect of miR-210 on the cell cycle (Fig. 2D). Transfection of miR-210 resulted in a significant increase in the proportion of cells in G_1/G_0 phase as well as a significant decrease in the proportion of cells in S phase, whereas the proportion of cells in G_2/M phase was unaltered. These results indicate that miR-210 induces cell cycle arrest in both G_1/G_0 and G_2/M phases because cell cycle arrest only in G_1/G_0 phase decreases the proportion of cells in G_2/M phase. In addition, overexpression of miR-210 resulted in a significant increase in the proportion of FITC-annexin V-positive cells (Fig. 2E, upper right and lower right) and FITC-annexin V-negative/propidium iodide (PI)-positive cells (Fig. 2E, upper left), and a significant decrease in the proportion of FITC-annexin V-negative/PI-negative cells (Fig. 2E, lower left), which indicated that overexpression of miR-210 may lead to apoptosis and necrosis. Taken together, the results suggest that miR-210 may inhibit proliferation of ESCC cells mainly by inducing cell cycle arrest and apoptosis.

Identification of Candidate Target Genes Degraded by miR-210—To investigate the molecular mechanism by which miR-210 inhibits ESCC cell proliferation, we analyzed the target genes of miR-210 in ESCC. We performed comprehen-

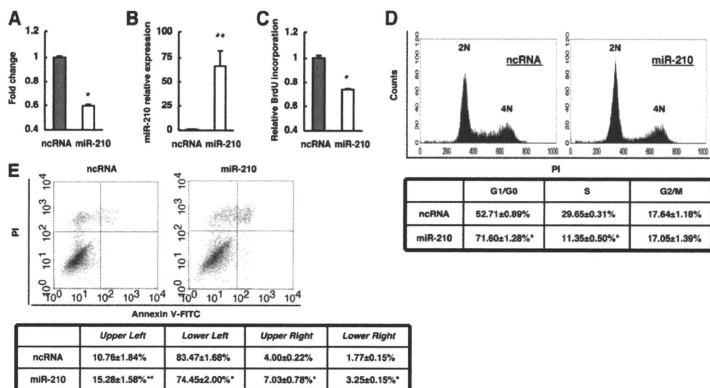


FIGURE 2. Functions of miR-210 in KYSE-170 cells. A, effect of miR-210 on cell proliferation was investigated by the WST-1 assay. Cells were incubated for 48 h after transfection with either ncRNA or miR-210, and viability was evaluated. The values are shown relative to the value obtained with ncRNA. B, expression levels of miR-210 in cells at 48 h after transfection with either ncRNA or miR-210 were investigated by qRT-PCR. The values are shown relative to the value obtained with ncRNA. C, 48 h after transfection, cell proliferation was evaluated by BrdU incorporation. The values are shown relative to the value obtained with ncRNA. D, effects of miR-210 on the cell cycle were investigated. The PI-stained DNA content of the cells was evaluated using a FACScan flow cytometer at 48 h after transfection. E, at 48 h after transfection, cells were stained with FITC-conjugated annexin V, and PI and cell death was evaluated using a FACScan flow cytometer. $n = 3$; **, $p < 0.05$; *, $p < 0.01$ versus ncRNA.

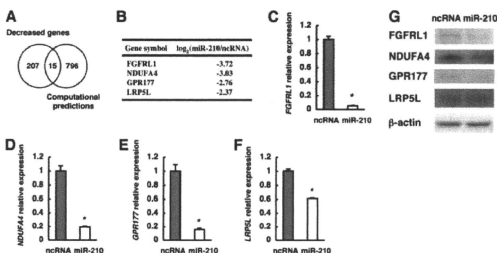


FIGURE 3. Identification of candidate target genes degraded by miR-210 in KYSE-170 cells. A, Venn diagram showing overlapping sets of genes whose expression was decreased >5-fold by transfection of miR-210 and computationally predicted target genes of miR-210. B, list of four potential miR-210 target genes with a signal value of more than 50 in ncRNA-transfected cells upon microarray analysis. C-F, expression levels of the four potential miR-210 target mRNAs assessed by qRT-PCR. The values are shown relative to the value obtained with ncRNA ($n = 3$; *, $p < 0.01$). G, Western blot analyses of FGFR1, NDUFA4, GPR177, LRP5L, and β -actin proteins.

single transcriptome analysis using RNA from ESCC cells transfected with either ncRNA or miR-210. Assuming that the expression of target genes of miR-210 might be down-regulated in cells transfected with miR-210, we selected 222 genes whose expression was decreased by more than 5-fold in miR-210-transfected cells compared with ncRNA-transfected cells (supplemental Table 2). Fifteen of the 222 genes were predicted to be miR-210 target genes by the target prediction

programs microcosm (2), TargetScan (19), and PicTar (20) (Fig. 3A and supplemental Tables 2 and 3). Four (FGFR1, NDUFA4, GPR177, and LRP5L) of these 15 genes had a signal value of more than 50 in ncRNA-transfected cells (Fig. 3B and supplemental Table 2). Furthermore, their expression was confirmed by qRT-PCR and Western blotting; the mRNA expression of all four genes was significantly down-regulated by transfection of miR-210, although the degree of decrease of

MicroRNA-210 Regulates Cancer Cell Cycle and Death

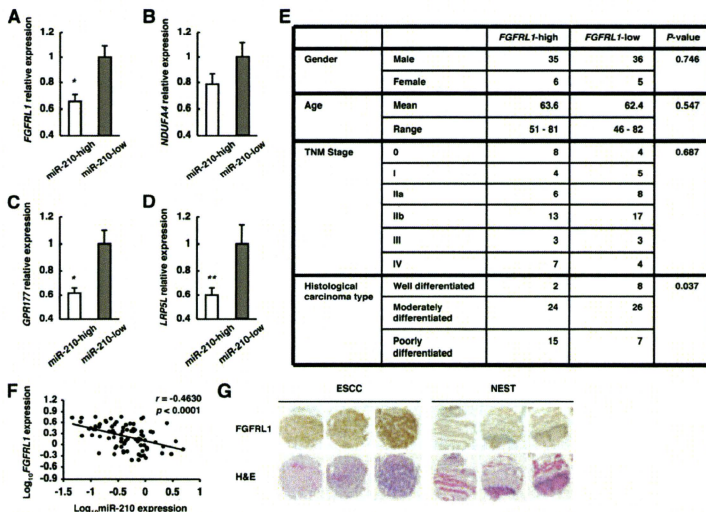


FIGURE 4. Identification of candidate target genes of miR-210 in ESCC. **A–D**, *FGFR1*, *NDUFA4*, *GPR177*, and *LRP5L* expression levels in ESCCs divided into two groups on the basis of miR-210 expression levels were assessed by qRT-PCR. The values are shown relative to the value obtained for the miR-210-low group ($n = 41$; **, $p < 0.05$, * $p < 0.01$). **E**, Clinicopathologic characteristics of 82 ESCCs divided into two groups ($n = 41$) on the basis of *FGFR1* expression levels. **F**, plot of \log_{10} *FGFR1* relative expression intensity against \log_{10} miR-210 relative expression intensity. The line represents an approximated curve. The correlation coefficient (r) and the p value indicate the statistical significance of the negative correlation between the x and y variables. **G**, Immunohistochemistry for *FGFR1* on ESCC and NEST. These sections were stained by anti-*FGFR1* antibody and by hematoxylin and eosin (H&E).

LRP5L was somewhat low (Fig. 3, C–F). The expression levels of *FGFR1*, *NDUFA4*, and *GPR177* proteins were also down-regulated by transfection of miR-210 (Fig. 3G). Meanwhile, the expression levels in *LRP5L* protein showed no change at 48 h after transfection of miR-210 (Fig. 3G). To validate these genes as targets of miR-210 further, we examined their expression in clinical ESCC samples. Of the four genes, the expression of *FGFR1*, *GPR177*, and *LRP5L* was significantly down-regulated in the miR-210-high group compared with the miR-210-low group (Fig. 4, A, C, and D), whereas *NDUFA4* was not significantly different between the two groups (Fig. 4B). We then divided the 82 ESCC samples into two groups ($n = 41$) on the basis of their *FGFR1*, *GPR177*, or *LRP5L* expression levels and compared the two groups in terms of their clinicopathologic characteristics. A significant association with histological type was observed for the *FGFR1*-classified groups (Fig. 4E), but not for the *GPR177*- or *LRP5L*-classified ones (data not shown), which agrees well with the finding that a decrease in miR-210 expression correlates well with the poorly differentiated state of ESCC. A statistically significant negative correlation was obtained between

expression levels of miR-210 and that of *FGFR1* in ESCC (Fig. 4F). Furthermore, sections of ESCC and NEST were stained by immunohistochemistry for *FGFR1*. The results indicated that *FGFR1* protein is expressed in ESCC and the expression levels are enhanced compared with NEST (Fig. 4G).

MIR-210 Targets *FGFR1* 3'-UTR Directly—Five sites in the *FGFR1* 3'-UTR are predicted to be potential target sites of miR-210 by microcosm (Fig. 5A), although none of them is conserved across species such as mouse, rat, and chicken. To examine whether *FGFR1* is a direct target of miR-210, we cloned the 3'-UTR of *FGFR1* into a pGL3-Luc vector (pGL3-Luc-*FGFR1* 3'-UTR) to perform reporter assay. When miR-210 was transfected into the cells with this reporter construct but not the mock, luciferase activity was repressed more than 50% compared with transfection of ncRNA (Fig. 5B). Meanwhile, luciferase activities in cells transfected with reporter constructs containing the 3'-UTR of *WSB2* or *GD12* were not repressed by the transfection of miR-210 (Fig. 5B). *WSB2* and *GD12* were not included in either predicted target genes of miR-210 or 222 genes decreased in miR-210-transfected cells (supplemental Tables 2 and 3). These results suggest that

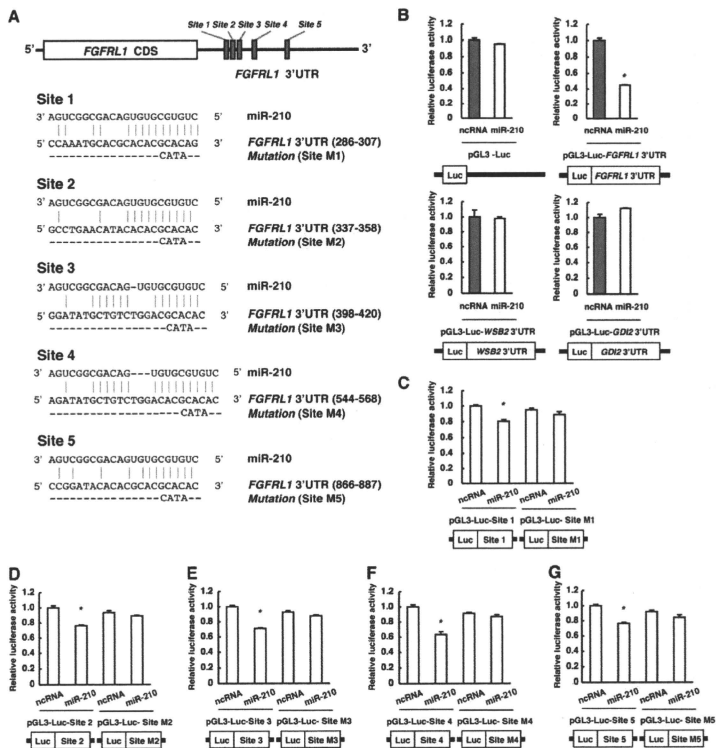


FIGURE 5. Identification of miR-210 target sites in *FGFR1* 3'-UTR. A, schematic diagram of potential miR-210-target sites in *FGFR1* 3'-UTR. B-G, cells were transfected with either ncRNA or miR-210 at 24 h after transfection with the pGL3 luciferase expression vector containing 3'-UTR of each gene or candidate miR-210 target site in *FGFR1* 3'-UTR. After 14 h, reporter luciferase activity was evaluated. The values are shown relative to the value obtained with ncRNA ($n = 3$; $p < 0.01$).

FGFR1 is a direct and robust target gene of miR-210 in ESCC. For further analysis, we cloned the each putative miR-210-target site or its point mutant in sequences corresponded to "seed sequence" of miR-210 into a pGL3-Luc vector (Fig. 5A) and performed reporter assays (Fig. 5, C-G). When miR-210 was transfected into the cells, luciferase activity was significantly repressed in all five sites. By contrast, when mutation was introduced in these sites, the repressions by miR-210

were completely abolished in all cases (Fig. 5, C-G). These results suggested that these five sites in the *FGFR1* 3'-UTR are target sites of miR-210.

FGFR1 Accelerates Cancer Cell Proliferation by Preventing Cell Cycle Arrest in G_1/G_0 .—To investigate the roles of *FGFR1* in cancer cell proliferation, we first examined the effect of *FGFR1* knockdown by using two types of *FGFR1* siRNA. With both siRNAs, knockdown of *FGFR1* significantly de-

MicroRNA-210 Regulates Cancer Cell Cycle and Death

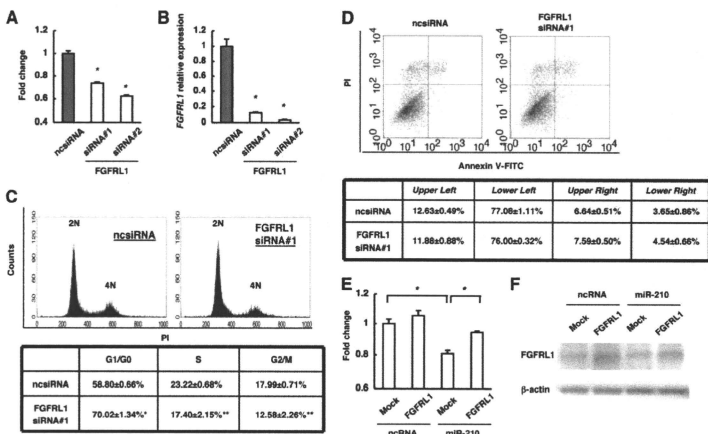


FIGURE 6. Functions of FGFR1 in KYSE-170 cells. *A*, effect of *FGFR1* on cell proliferation was investigated by the WST-1 assay. Cells were incubated for 48 h after transfection with ncsiRNA, *FGFR1* siRNA#1 or 2, and viability was evaluated. The values are shown relative to the value obtained with ncsiRNA ($n = 3$; $^* p < 0.01$ versus ncsiRNA). *B*, *FGFR1* expression levels in *A* were assessed by qRT-PCR. The values are shown relative to the value obtained with ncsiRNA ($n = 3$; $^* p < 0.01$ versus ncsiRNA). *C*, effects of *FGFR1* knockdown on the cell cycle were investigated. The PI-stained DNA content of the cells was evaluated using a FACScan flow cytometer at 48 h after transfection ($n = 3$; $^* p < 0.05$; $^{**} p < 0.01$ versus ncsiRNA). *D*, at 48 h after transfection, cells were stained with FITC-conjugated annexin V and PI, and cell death was evaluated using a FACScan flow cytometer ($n = 3$). *E*, cells were transfected with either ncsiRNA or miR-210 at 24 h after transfection with the *FGFR1* expression vector or mock. After 48 h, viability was evaluated. The values are shown relative to the value obtained with ncsiRNA and mock transfection ($n = 3$; $^* p < 0.01$). *F*, Western blot analyses of *FGFR1* and β -actin proteins in *E* are shown.

creased proliferation of ESCC cells, whereas a ncsiRNA had no inhibitory effect (Fig. 6A). The level of *FGFR1* expression was reduced to ~10% of the original level with both siRNAs (Fig. 6B). Next, we examined the effects of *FGFR1* knockdown on the cell cycle (Fig. 6C). Knockdown of *FGFR1* resulted in a significant increase in the proportion of cells in G_1/G_0 phase and a decrease in that in G_2/M phases. These results indicated that down-regulation of *FGFR1* induced cell cycle arrest in G_1/G_0 . Down-regulation of *FGFR1* did not significantly change the proportions of FITC-annexin V-positive cells, FITC-annexin V-negative/PI-positive cells, and FITC-annexin V-negative/PI-negative cells, which indicated that *FGFR1* is not involved in apoptosis and necrosis (Fig. 6D). In contrast, overexpression of *FGFR1* with no 3'-UTR significantly reduced the inhibitory effect of miR-210 on cell proliferation (Fig. 6E). Then, expression levels of *FGFR1* proteins are actually increased in cells transfected with a *FGFR1* expression vector without the 3'-UTR of *FGFR1* (Fig. 6F). These findings suggest that *FGFR1* increases the proliferation of ESCC cells by inhibiting cell cycle arrest in G_1/G_0 phase.

Endogenous miR-210 Regulates Expression Levels of *FGFR1* and Cancer Cell Proliferation—To examine whether endogenous miR-210 regulates the expression levels of endog-

enous *FGFR1*, we examined the effect of anti-miR-210 in KYSE-590 cells, which relatively highly expresses miR-210. The treatment by 2'-*O*-methylated antisense RNA of miR-210 significantly enhanced the expression levels of *FGFR1* mRNA and protein (Fig. 7A). Then, cancer cell proliferation was significantly increased (Fig. 7B). These results may indicate that miR-210 endogenously regulates the expression levels of *FGFR1* and cancer cell proliferation.

DISCUSSION

In the present study, we showed for the first time that expression of miR-210 is down-regulated in ESCC cell lines as well as in clinical samples and that miR-210 induces cell cycle arrest and apoptosis *in vitro*, thus inhibiting the proliferation of cancer cells. Furthermore, we found that not only miR-210 expression was decreased in ESCC, but the degree of tumor differentiation corresponded well with the levels of miR-210 in clinical ESCC samples; thus, more poorly differentiated ESCCs exhibited less miR-210 expression. The results indicate that the level of miR-210 expression may serve as a clinical marker for the degree of tumor differentiation *in vivo*. We also examined whether the lower levels of miR-210 expression in poorly differentiated ESCC were related to the enhanced

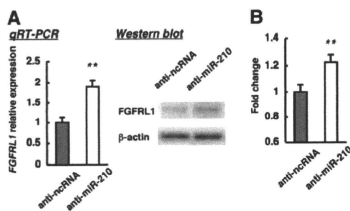


FIGURE 7. Effects of functional inhibition of endogenous miR-210. A, effect of inhibition of endogenous miR-210 on *FGFR1* expression levels was assessed by qRT-PCR and Western blot analyses using KYSE-590 cells. Cells were incubated for 48 h after transfection with anti-ncRNA or anti-miR-210. The values are shown relative to the value obtained with anti-ncRNA ($n = 3$; **, $p < 0.05$ versus anti-ncRNA). B, cell viability in A was evaluated by the WST-1 assay. The values are shown relative to the value obtained with anti-ncRNA ($n = 3$; **, $p < 0.05$ versus anti-ncRNA).

proliferation of such carcinomas, and we found that miR-210 acts as a tumor-suppressive miRNA in ESCC.

In contrast to our study, miR-210 was reported to be up-regulated in breast cancer, pancreatic tumors, and head and neck cancer and to be correlated with their poor outcome (21–24). Moreover, previous studies have shown that miR-210 inhibits apoptosis and bypasses cell cycle arrest in cancer cell lines such as MCF-7 and HCT116 Dicer^{+/+} cells (25, 26). Thus, our finding appears to be different from the previous reports that miR-210 is up-regulated in cancer tissues and enhances cell survival. The reason for this apparent discrepancy is uncertain. A likely explanation in the function of miR-210 is that it is possible that the expression of miR-210 might only reflect the hypoxia status in these cases as a surrogate marker for tumor hypoxia because miR-210 is the most robustly induced miRNA under hypoxia (9, 25, 26). Additionally, the apparently discrepant results in cancer cell lines might be explained by cell type-specific differences in the expression levels of target genes of miR-210. The results of our transcriptome analysis on ESCC cells that expressed miR-210 ectopically supported this possibility because induction of miR-210 did not affect the expressions of *CASPRA2* and *MNT* (supplemental Table 2), which are target genes of miR-210 and induce apoptosis and cell cycle arrest, respectively (26, 27). Similar to our findings, Huang *et al.* have reported recently that miR-210 represses the initiation of tumor growth when human head and neck or pancreatic tumor cell lines that are expressing miR-210 ectopically are implanted into immunodeficient mice (10).

In the present study, we found that miR-210 is targeted to the *FGFR1* 3'-UTR and suppresses *FGFR1* expression in ESCC. Five sites in the 3'-UTR of *FGFR1* were identified as target sites of miR-210. The repression in the *FGFR1* 3'-UTR containing these five sites was considerably larger than that in each miR-210 target sites. These five miR-210 target sites in the *FGFR1* 3'-UTR may function synergistically in the decrease in the *FGFR1* expression level. It has been actually reported that closely located multiple miRNA

target sites in the 3'-UTR of a gene may function synergistically (28, 29). As suggested by the observation that overexpression of miR-210 in ESCC cells down-regulated expression of *FGFR1* more than that of the other predicted target genes, we found that *FGFR1* mRNA expression was down-regulated in the miR-210-high group of clinical samples and that the level of expression was correlated inversely with the degree of differentiation. Moreover, knockdown of *FGFR1* by siRNA inhibited ESCC cell proliferation, whereas overexpression of *FGFR1* effectively rescued the miR-210-induced suppression of ESCC cell proliferation. Together, these findings show that miR-210 might exert its tumor-suppressive effect in ESCC mainly by targeting *FGFR1*. This conclusion was supported by a recent study showing that *FGFR1* could partially rescue the phenotype (suppression of tumor growth) caused by ectopic expression of miR-210 in tumor xenografts (10). However, targeting of *FGFR1* by miR-210 appears to explain only part of the action of miR-210: down-regulation of *FGFR1* arrested the cell cycle in G₁/G₀ phase, but not in G₂/M phase, although miR-210 induced cell cycle arrest in both phases. Hence, miR-210-induced cell cycle arrest in G₂/M phase and apoptosis might be regulated by other targets of miR-210. In fact, our transcriptome analysis identified several genes whose expression was regulated differentially by miR-210. Further studies are clearly required to understand fully the molecular mechanism of tumor suppression by miR-210.

In conclusion, the results of our present study show that miR-210 inhibits the proliferation of ESCC cells by inducing cell cycle arrest and apoptosis and that the effects of miR-210 are mediated mainly by the targeting of *FGFR1*. Our data suggest that down-regulation of miR-210 might play an important role in the proliferation of ESCC and that miR-210 and *FGFR1* might serve as clinical markers for tumor differentiation and therapeutic targets of ESCC.

Acknowledgments—We thank T. Murali, K. Kodama and S. Yoshino for technical assistance.

REFERENCES

1. Tsuchiya, S., Okuno, Y., and Tsujimoto, G. (2006) *J. Pharmacol. Sci.* **101**, 267–270
2. Griffiths-Jones, S., Grocock, R. J., van Dongen, S., Bateman, A., and Enright, A. J. (2006) *Nucleic Acids Res.* **34**, D140–D144
3. Tsuchiya, S., Oka, M., Imanaka, Y., Kunimoto, R., Okuno, Y., Terawata, K., Sato, F., Tsujimoto, G., and Shimizu, K. (2009) *Nucleic Acids Res.* **37**, 3821–3827
4. Volinia, S., Calin, G. A., Liu, C. G., Ambs, S., Cimmino, A., Petrocca, F., Visone, R., Iorio, M., Roldo, C., Ferracin, M., Prueitt, R., Yanaihara, N., Lanza, G., Scarpa, A., Vecchione, A., Negrini, M., Harris, C. C., and Croce, C. M. (2006) *Proc. Natl. Acad. Sci. U.S.A.* **103**, 2257–2261
5. Zavadil, J., Narasimhan, M., Blumenberg, M., and Schneider, R. J. (2007) *Cells Tissues Organs* **185**, 157–161
6. Dow, L. E., Elsum, I. A., King, C. L., Kinross, K. M., Richardson, H. E., and Humbert, P. O. (2008) *Oncogenes* **27**, 5988–6001
7. Joshi, J., Fernandez-Marcos, P. J., Galvez, A., Amarny, R., Linares, J. F., Duran, A., Pathrose, P., Leitges, M., Calamero, M., Collado, M., Salas, C., Serrano, M., Moscat, J., and Diaz-Meco, M. T. (2008) *EMBO J.* **27**, 2181–2193
8. Karp, C. M., Tan, T. T., Mathew, R., Nelson, D., Mukherjee, C., Degen-

MicroRNA-210 Regulates Cancer Cell Cycle and Death

- hardt, K., Karantzis-Wadsworth, V., and White, E. (2008) *Cancer Res* **68**, 4105–4115
9. Giannakakis, A., Sandidzopoulos, G., Gresbeck, J., Liang, S., Huang, J., Hasegawa, K., Li, C., O'Brien-Jenkins, A., Kataros, D., Weber, R. L., Simon, C., Coukos, G., and Zhang, L. (2008) *Cancer Biol. Ther.* **7**, 255–264
10. Huang, X., Ding, L., Bennewith, K. L., Tong, R. T., Welford, S. M., Ang, K. K., Story, M., Le, Q. T., and Giaccia, A. J. (2009) *Mol. Cell* **35**, 856–867
11. Isohata, N., Aoyagi, K., Mabuchi, T., Daiko, H., Fukaya, M., Ohta, H., Ogawa, K., Yoshida, T., and Sasaki, H. (2009) *Int. J. Cancer* **125**, 1212–1221
12. Thépot, A., Hautefeuille, A., Cros, M. P., Abedi-Ardekani, B., Pétrel, A., Damour, O., Krutovskikh, V., and Hainaut, P. (2010) *Int. J. Cancer* **127**, 2051–2062
13. Sobin, L., and Wittkeind, C. (2002) *TNM Classification of Malignant Tumors*, 6th Ed, pp. 60–64, John Wiley and Sons, New York
14. Ito, T., Shimada, Y., Kan, T., David, S., Cheng, Y., Mori, Y., Agarwal, R., Paun, B., Jin, Z., Olanu, A., Hamilton, J. P., Yang, J., Abraham, J. M., Meltzer, S. J., and Sato, F. (2008) *Cancer Res* **68**, 3214–3224
15. Tanaka, E., Hashimoto, Y., Ito, T., Kondo, K., Higashiyama, M., Tsunoda, S., Ortiz, C., Sakai, Y., Inazawa, J., and Shimada, Y. (2007) *Clin. Cancer Res* **13**, 1331–1340
16. Mathé, E. A., Nguyen, G. H., Bowman, E. D., Zhao, Y., Budhu, A., Schetter, A. J., Bruun, R., Reimers, M., Kumamoto, K., Hughes, D., Altorki, N. K., Casson, A. G., Liu, C. G., Wang, X. W., Yanahara, N., Hagiwara, N., Dannenberg, A. J., Miyashita, M., Croce, C. M., and Harris, C. C. (2009) *Clin. Cancer Res* **15**, 6192–6200
17. Ogawa, R., Ishiguro, H., Kuwabara, Y., Kimura, M., Mitsui, A., Katada, T., Harata, K., Tanaka, T., and Fujii, Y. (2009) *Med. Mol. Morphol.* **42**, 102–109
18. Hino, K., Tsuchiya, K., Fukao, T., Kiga, K., Okamoto, R., Kanai, T., and Watanabe, M. (2008) *RNA* **14**, 1433–1442
19. Lewis, B. P., Shih, I. H., Jones-Rhoades, M. W., Bartel, D. P., and Burge, C. B. (2003) *Cell* **115**, 787–798
20. Lall, S., Grün, D., Krek, A., Chen, K., Wang, Y. L., Dewey, C. N., Soed, P., Colombo, T., Bray, N., Macmenamin, P., Kao, H. L., Gunsalus, K. C., Pachter, L., Piano, F., and Rajewsky, N. (2006) *Curr. Biol.* **16**, 460–471
21. Fockens, J. A., Stiewerts, A. M., Smid, M. P., de Weerd, V., Boersma, A. W., Klijn, J. G., Wiemer, E. A., and Martens, J. W. (2008) *Proc. Natl. Acad. Sci. U.S.A.* **105**, 13021–13026
22. Camps, C., Buffa, F. M., Colella, S., Moore, J., Sottirou, C., Sheldon, H., Harris, A. L., Gleslie, J. M., and Ragoissis, I. (2008) *Clin. Cancer Res.* **14**, 1340–1348
23. Greither, T., Grochala, L. F., Udelnow, A., Lautenschläger, C., Würfl, P., and Taubert, H. (2010) *Int. J. Cancer* **126**, 73–80
24. Gee, H. E., Camps, C., Buffa, F. M., Patiar, S., Winter, S. C., Betts, G., Hester, J., Corbridge, R., Cox, C., West, C. M., Ragoissis, J., and Harris, A. L. (2010) *Cancer* **116**, 2148–2158
25. Kulshreshtha, R., Ferracin, M., Wojcik, S. E., Garzon, R., Alder, H., Agosto-Perez, F. J., Davuluri, R., Liu, C. G., Croce, C. M., Negrini, M., Calin, G. A., and Ivan, M. (2007) *Mol. Cell. Biol.* **27**, 1859–1867
26. Zhang, Z., Sun, H., Dai, H., Walsh, R. M., Imakura, M., Schelter, J., Burchar, J., Dai, X., Chang, A. N., Diaz, R. L., Marszalek, J. R., Bartz, S. R., Carleton, M., Cleary, M. A., Linsley, P. S., and Grandori, C. (2009) *Cell Cycle* **8**, 2756–2768
27. Kim, H. W., Haider, H. K., Jiang, S., and Ashraf, M. (2009) *J. Biol. Chem.* **284**, 33161–33168
28. Grimson, A., Farh, K. K., Johnston, W. K., Garrett-Engle, P., Lim, L. P., and Bartel, D. P. (2007) *Mol. Cell* **27**, 91–105
29. Rajewsky, N. (2006) *Nat. Genet.* **38**, S8–S13

Supplementary Table 1. List of primers used for real-time PCR analysis

Gene Symbol	Forward (5' -> 3')	Reverse (5' -> 3')
<i>FGFRL1</i>	acacagccctccaagatgag	gcaggtcttcaggetcagt
<i>NDUFA4</i>	agcttgatccctctttgt	ctggacgttccttctcagc
<i>GPR177</i>	aggcatctatgggatgtgga	ggaatattcgaagcgetga
<i>LRP5L</i>	ctcaaagctgtgaacgtgga	gcggctctactggtgaagac
<i>GAPDH</i>	gagtcaacggattggtcgt	ttgatttggagggatctcg

Gene Symbol	description	ncRNA	miR-210	Log ₂ (ratio)
<i>IGHG3</i>	Immunoglobulin heavy chain C gene segment [Source:IMG/GENE-DB;Acc:IGHG3]	41	1	-5.36
	NADH-cytochrome b5 reductase (EC 1.6.2.2) (H5R) (Diaphorase-1) (cytochrome b5 reductase 3) contains NADH-cytochrome b5 reductase membrane bound form; NADH-cytochrome b5 reductase soluble form. [Source:Uniprot/SWISSPROT;Acc:P00387]	40	1	-5.32
<i>CYB5B3</i>		39	1	-5.29
<i>FAM194A</i>	[Source:Uniprot/SWISSPROT;Acc:Q96LR4]	37	1	-5.21
<i>COBL</i>	Protein cordon-bleu. [Source:Uniprot/SWISSPROT;Acc:Q75128]	37	1	-5.21
	Bone marrow stromal antigen 2 precursor (BST-2) (CD317 antigen) (HMI 24 antigen). [Source:Uniprot/SWISSPROT;Acc:Q10889]	35	1	-5.13
<i>BST2</i>		35	1	-5.13
<i>ONCO_HUMAN</i>	Oncomodulin (Om) (Parvalbumin beta). [Source:Uniprot/SWISSPROT;Acc:P29290]	35	1	-5.13
	POU domain, class 3, transcription factor 1 (Octamer-binding transcription factor 6) (Oct-6) (POU domain transcription factor SC1P). [Source:Uniprot/SWISSPROT;Acc:Q03052]	35	1	-5.13
<i>POU3F1</i>		34	1	-5.09
<i>PTPRT</i>	Receptor-type tyrosine-protein phosphatase 1 precursor (EC 3.1.3.48) (R-PTP-1) (RPTP-rho). [Source:Uniprot/SWISSPROT;Acc:Q14521]	35	1	-5.09
	Prominin-1 precursor (Prominin-like protein 1) (Antigen AC133) (CD133 antigen). [Source:Uniprot/SWISSPROT;Acc:Q43490]	33	1	-5.04
<i>PROM1</i>				
	(Aminopeptidase P1L5) (Paromycin-insensitive leucyl-specific aminopeptidase) (P1L5-AP) (Type 1 tumor necrosis factor receptor shedding aminopeptidase regulator). [Source:Uniprot/SWISSPROT;Acc:Q9NZ08]	29	1	-4.86
<i>ARTS1_HUMAN</i>		28	1	-4.81
<i>Q96I54_HUMAN</i>		28	1	-4.81
<i>CALN1</i>	Calnexin-1 (Calcium-binding protein CaBP8) [Source:Uniprot/SWISSPROT;Acc:Q9BXU9]	28	1	-4.81
	UDP-glycosyltransferase 2B4 precursor (EC 2.4.1.17) (UDPGT1) (Hydroxycycloic acid) (HLUG25) (UDPGLT1). [Source:Uniprot/SWISSPROT;Acc:P06133]	27	1	-4.75
<i>UGT2B4</i>				
	Gamma-aminobutyric-acid receptor subunit beta-1 precursor (GABA(A) receptor subunit beta-1). [Source:Uniprot/SWISSPROT;Acc:P18505]	26	1	-4.7
<i>GABRB1</i>				
	DNA fragmentation factor subunit beta (EC 3.-.-) (DNA fragmentation factor 40 kDa subunit) (DF-40) (Caspase-activated deoxyribonuclease 1) (Caspase-activated DNase) (CAD) (Caspase-activated nuclease) (CDAN). [Source:Uniprot/SWISSPROT;Acc:Q76075]	26	1	-4.7
<i>DFEB</i>				
	Gamma-aminobutyric-acid receptor subunit delta precursor (GABA(A) receptor subunit delta). [Source:Uniprot/SWISSPROT;Acc:Q14764]	26	1	-4.7
<i>GABRD</i>				
<i>Q5LV99_HUMAN</i>		25	1	-4.64
<i>MANEAL</i>	mannosidase, endo-alpha-like isoform 2 [Source:RefSeq_peptide;Acc:NP_689709]	25	1	-4.64
	Multiple epidermal growth factor-like domains 6 precursor (EGF-like domain-containing protein 3) (Multiple EGF-like domain protein 3). [Source:Uniprot/SWISSPROT;Acc:Q75095]	24	1	-4.58
<i>MEGF6</i>				
	Metalloprotease inhibitor 4 precursor (TIMP-4) (Tissue inhibitor of metalloproteinases 4). [Source:Uniprot/SWISSPROT;Acc:Q99721]	23	1	-4.52
<i>TIMP4</i>				
	Tumor necrosis factor-inducible protein TSG-6 precursor (TNF-stimulated gene 6 protein) (Hyaluronate-binding protein). [Source:Uniprot/SWISSPROT;Acc:P98066]	23	1	-4.52
<i>TNFAIP6</i>				
	Interleukin-24 precursor (Suppression of tumorigenicity 16 protein) (Melanoma differentiation-associated gene 7 protein) (MDA-7). [Source:Uniprot/SWISSPROT;Acc:Q13007]	23	1	-4.52
<i>IL24</i>				
<i>Q8NHA6_HUMAN</i>		23	1	-4.52
	Seven transmembrane helix receptor. [Source:Uniprot/SPTREMBL;Acc:Q8NHA6]	23	1	-4.52
<i>PDE1B</i>	Calcium/calmodulin-dependent 3'-5' cyclic nucleotide phosphodiesterase 1B (EC 3.1.4.17) (Cam-PDE 1B) (65 kDa Cam-PDE). [Source:Uniprot/SWISSPROT;Acc:Q00164]	23	1	-4.52
	Signal-induced proliferation-associated protein 1 (Spa-1) (GTPase-activating protein Spa-1) (p130 SPA-1). [Source:Uniprot/SWISSPROT;Acc:Q96F54]	22	1	-4.46
<i>EHBP1L1</i>		43	2	-4.43
<i>C14orf174</i>	C14orf174 protein. [Source:Uniprot/SPTREMBL;Acc:Q2M3P3]	43	2	-4.43
	[Source:Uniprot/SWISSPROT;Acc:Q9ULL1]	21	1	-4.39
<i>PLEKHG1</i>				
<i>ASTN1</i>	Astrotactin-1 precursor. [Source:Uniprot/SWISSPROT;Acc:Q14525]	20	1	-4.32
	Pregnancy-specific beta-1-glycoprotein 1 precursor (PSBG-1) (Pregnancy-specific beta-1 glycoprotein C7) (PS-beta-C7) (fetal liver non-specific cross-reactive antigen 12) (FL-NC1A-12) (PSG95) (CD66f antigen). [Source:Uniprot/SWISSPROT;Acc:P11464]	20	1	-4.32
<i>PSG1</i>				
<i>SLC6A20</i>	Sodium- and chloride-dependent transporter XTRP3 (Solute carrier family 6 member 20) (Neurotransmitter transporter h21A homolog). [Source:Uniprot/SWISSPROT;Acc:Q9NP91]	20	1	-4.32
	Leucine-rich repeat neuronal protein 1 precursor (Neuronal leucine-rich repeat protein 1) (NLRR-1). [Source:Uniprot/SWISSPROT;Acc:Q9UXX5]	39	2	-4.29
<i>LRRN1</i>				
<i>IFT57</i>	estrogen-related receptor beta like 1 [Source:RefSeq_peptide;Acc:NP_060480]	19	1	-4.25
	CDNA FLJ25404 fis. clone T102888 (Hypothetical protein FLJ25404). [Source:Uniprot/SPTREMBL;Acc:Q96L31]	19	1	-4.25
<i>Q96L31_HUMAN</i>				
<i>COCH</i>	Cochlin precursor (COCH-5B2). [Source:Uniprot/SWISSPROT;Acc:Q43405]	19	1	-4.25
<i>NP_683707.2</i>	GREB1 protein Isoform B [Source:RefSeq_peptide;Acc:NP_149081]	19	1	-4.25
<i>Q8NAW6_HUMAN</i>	CDNA FLJ34651 fis. clone KIDNE2018167. [Source:Uniprot/SPTREMBL;Acc:Q8NAW6]	19	1	-4.25
	IFAF6-like RNA polymerase II p300/CBP-associated factor-associated factor 65 kDa subunit 6L (PCF4-associated factor 65-alpha) (PAF65-alpha). [Source:Uniprot/SWISSPROT;Acc:Q9Y6J9]	18	1	-4.17
<i>TAF6L</i>				
	transmembrane protease, serine 12 [Source:RefSeq_peptide;Acc:NP_072385]	18	1	-4.17
<i>TMPSK12</i>				
<i>Q8NAT4_HUMAN</i>	CDNA FLJ34815 fis. clone NT2NE007786. [Source:Uniprot/SPTREMBL;Acc:Q8NAT4]	17	1	-4.09
	Solute carrier family 12 member 3 (Thiazide-sensitive sodium-chloride cotransporter) (Na-Cl symporter). [Source:Uniprot/SWISSPROT;Acc:P55017]	17	1	-4.09
<i>SLC12A3</i>				
	Cell adhesion molecule-related down-regulated by oncogenes precursor. [Source:Uniprot/SWISSPROT;Acc:Q4KMG1]	17	1	-4.09
<i>CDON</i>				
<i>SGCG</i>	Gamma-sarcoglycan (Gamma-SG) (35 kDa dystrophin-associated glycoprotein) (35DA(G)). [Source:Uniprot/SWISSPROT;Acc:Q13326]	17	1	-4.09
<i>DCDC2</i>	[Source:Uniprot/SWISSPROT;Acc:Q9UHG0]	17	1	-4.09

Gene Symbol	Description	ncRNA	miR-210	Log ₂ (ratio)
	Pancreas transcription factor 1 subunit alpha (Pancreas-specific transcription factor 1a) (bHLH transcription factor p48) (p48 DNA-binding subunit of transcription factor PTF1) (PTF1-p48). [Source:Uniprot/SWISSPROT:Acc:Q7RTS3]			
<i>PTF1A</i>		34	2	-4.09
<i>IGSF5</i>	IGSF5 protein (Fragment). [Source:Uniprot/SPTREMBL:Acc:Q9NS15]	17	1	-4.09
<i>TECTA</i>	Alpha-tectorin precursor. [Source:Uniprot/SWISSPROT:Acc:Q75433]	17	1	-4.09
	Leucine-rich repeat and transmembrane domain-containing protein 2 precursor. [Source:Uniprot/SWISSPROT:Acc:Q9N967]			
<i>LRTM2</i>		16	1	-4
	Myelin transcription factor 1-like protein (MyT1L protein) (MyT1L). [Source:Uniprot/SWISSPROT:Acc:Q9UL68]			
<i>MYT1L</i>		16	1	-4
<i>Q9JSH6_HUMAN</i>	CDNA: HJ 23429 fs, clone HRC 10578. [Source:Uniprot/SPTREMBL:Acc:Q9JSH6]	16	1	-4
<i>LKI</i>	Protein Irbh expression 1 homolog. [Source:Uniprot/SWISSPROT:Acc:Q9N4R5]	32	2	-4
<i>FSTL5</i>	Follistatin-related protein 5 precursor (Follistatin-like 5). [Source:Uniprot/SWISSPROT:Acc:Q9N475]	16	1	-4
<i>SEMG2</i>	Semenogelin-2 precursor (Semenogelin I) (SGII). [Source:Uniprot/SWISSPROT:Acc:Q02383]	15	1	-3.91
<i>Q16653-6</i>	[Source:RefSeq_peptide:Acc:NP_996536]	15	1	-3.91
<i>Q4VXH5_HUMAN</i>	XAGE-4 protein (Fragmen). [Source:Uniprot/SPTREMBL:Acc:Q8WWM0]	15	1	-3.91
<i>SERPINA2</i>	Alpha-1-antitrypsin-related protein precursor. [Source:Uniprot/SWISSPROT:Acc:P20848]	15	1	-3.91
<i>GSDMDC1</i>	Gasdermin domain-containing protein 1. [Source:Uniprot/SWISSPROT:Acc:P57764]	15	1	-3.91
<i>Q8TRU5_HUMAN</i>		14	1	-3.81
	Zinc finger protein 83 (Zinc finger protein HPF1). [Source:Uniprot/SWISSPROT:Acc:P51522]	14	1	-3.81
<i>ZNF83</i>				
	Lithostathine 1 alpha precursor (Pancreatic stone protein) (PSP) (Pancreatic thread protein) (PTP) (Islet of Langerhans regenerating protein) (REG) (Regenerating protein I alpha) (Islet cells regeneration factor) (ICRF). [Source:Uniprot/SWISSPROT:Acc:P05451]	14	1	-3.81
<i>REG1A</i>				
<i>GRP1</i>	[Source:Uniprot/SWISSPROT:Acc:Q9Y3R0]	28	2	-3.81
	Fibroblast growth factor receptor-like 1 precursor (FGF receptor-like protein 1) (Fibroblast growth factor receptor 5) (FGFR-like protein) (FGF homologous factor receptor). [Source:Uniprot/SWISSPROT:Acc:Q9N441]			
<i>FGFRL1</i>		277	21	-3.72
	Sex hormone-binding globulin precursor (SHBG) (Sex steroid-binding protein) (SBP) (Testis-specific androgen-binding protein) (ABP) (Testosterone-estrogen-binding globulin) (Testosterone-estradiol-binding globulin) (TeBG). [Source:Uniprot/SWISSPROT:Acc:P04278]			
<i>SHBG</i>		13	1	-3.7
	Peptidyl-prolyl cis-trans isomerase-like 2 (EC 5.2.1.8) (PPIase) (Rotamase) (Cyclophilin-60) (Cyclophilin-like protein Cyp-60). [Source:Uniprot/SWISSPROT:Acc:Q13356]			
<i>PP1L2</i>		13	1	-3.7
	Interleukin-21 precursor (IL-21) [Zell]. [Source:Uniprot/SWISSPROT:Acc:Q9HBE4]			
<i>IL21</i>		13	1	-3.7
	Chloride intracellular channel 6. [Source:Uniprot/SWISSPROT:Acc:Q96N71]			
<i>CLIC6</i>		13	1	-3.7
	SLIT and NTRK-like protein 2 precursor. [Source:Uniprot/SWISSPROT:Acc:Q9H156]			
<i>SLITRK2</i>		12	1	-3.58
	Regulating synaptic membrane exocytosis protein 1 (Rab3-interacting molecule 1) (RIM 1). [Source:Uniprot/SWISSPROT:Acc:Q861R5]			
<i>RIMS1</i>		12	1	-3.58
	Laylin precursor. [Source:Uniprot/SWISSPROT:Acc:Q6UX15]			
<i>LAYN</i>		12	1	-3.58
	Ankryin repeat and SOCS box protein 17 (ASH-17). [Source:Uniprot/SWISSPROT:Acc:Q9WX09]			
<i>ASB17</i>		12	1	-3.58
	Synaptobilin. [Source:Uniprot/SWISSPROT:Acc:Q15079]			
<i>RAD21L1</i>		12	1	-3.58
	Fibroblast growth factor 23 precursor (FGF-23) (Tumor-derived hypophosphatemia-inducing factor). [Source:Uniprot/SWISSPROT:Acc:Q9GZV9]			
<i>FGF23</i>		12	1	-3.58
	Calmodulin-binding transcription activator 1. [Source:Uniprot/SWISSPROT:Acc:Q9Y6Y1]			
<i>CAMTA1</i>		23	2	-3.52
	Apolipoprotein A-II precursor (Apo-AII) (ApoA-II) [Contains: Apolipoprotein A-II(1-76)]. [Source:Uniprot/SWISSPROT:Acc:P02652]			
<i>APOA2</i>		11	1	-3.46
	LOC 283537 protein (OTT1HUM0000018) [84]. [Source:Uniprot/SPTREMBL:Acc:Q6P9B3]			
<i>NP_861450.1</i>		11	1	-3.46
	NADH dehydrogenase [ubiquinone] 1 alpha subcomplex subunit 5 (EC 1.6.5.3) (EC 1.6.99.3) (NADH ubiquinone oxidoreductase 13 kDa B subunit) (Complex 1-13kD-B) (C1-13kD-B) (Complex I subunit B13). [Source:Uniprot/SWISSPROT:Acc:Q16718]			
<i>NDUFAS5</i>		11	1	-3.46
	D-aspartate oxidase (EC 1.4.3.1) (DASOX) (DDO). [Source:Uniprot/SWISSPROT:Acc:Q99489]			
<i>DDO</i>		22	2	-3.46
	BCoR-like protein 2 (BCL-6 corepressor-like protein 2). [Source:Uniprot/SWISSPROT:Acc:Q9N888]			
<i>BCORL2</i>		11	1	-3.46
	CDNA FLJ46365 fs, clone TEST14051054. [Source:Uniprot/SPTREMBL:Acc:Q6ZR18]			
<i>NM_207504</i>		11	1	-3.46
	major histocompatibility complex, class II, DP alpha I			
<i>IHA-DPA1</i>		22	2	-3.46
	Cyclin-dependent kinase inhibitor C (Cyclin-dependent kinase inhibitor p57) (p57KIP2). [Source:Uniprot/SWISSPROT:Acc:P49918]			
<i>CDKN1C</i>		11	1	-3.46
	Axonemal dynein light intermediate polypeptide 1 (Imer dynein arm light chain, axonemal) (hp28). [Source:Uniprot/SWISSPROT:Acc:Q14645]			
<i>DNAL1</i>		11	1	-3.46
	(MCH-2R) (MCH2) (G-protein coupled receptor 145) (GPR17). [Source:Uniprot/SWISSPROT:Acc:Q960V1]			
<i>MC1R2</i>		21	2	-3.39
	dynein heavy chain domain 3 [Source:RefSeq_peptide:Acc:NP_659298]			
<i>DNAH2</i>		21	2	-3.39
	Reticulon-2 (Neuroendocrine-specific protein-like 1) (NSP-like protein 1) (NSPL). [Source:Uniprot/SWISSPROT:Acc:Q75298]			
<i>RTN2</i>		21	2	-3.39
	[Source:Uniprot/SWISSPROT:Acc:P42127]			
<i>ASIP</i>		10	1	-3.32
	Amphiphysin. [Source:Uniprot/SWISSPROT:Acc:P49418]			
<i>AMPH</i>		10	1	-3.32
	F-box and leucine-rich repeat protein 21. [Source:RefSeq_peptide:Acc:NP_036291]			
<i>FBXL21</i>		10	1	-3.32
	[Source:Uniprot/SWISSPROT:Acc:Q9UKU9]			
<i>AWP112</i>		30	3	-3.32
<i>Q96RZ4_HUMAN</i>		30	3	-3.32
	C12orf50 protein (Fragment). [Source:Uniprot/SPTREMBL:Acc:Q6P674]			
<i>C12orf50</i>		20	2	-3.32

Supplementary Table 2. The list represents 222 genes decreased by more than five-fold in miR-210-transfected cells compared with ncRNA-transfected cells		ncRNA	miR-210	Log ₂ (ratio)
Gene Symbol	description			
<i>MSMB</i>	Beta-microglobulin precursor (Prostate secreted seminal plasma protein) (Prostate secretory protein PSP94) (PSP-94) (Seminal plasma beta-inhibin) (Immunoglobulin-binding factor) (IGBF) (PN44) [Source: Uniprot/SwissProt:Acc:P08118]	20	2	-3.32
<i>HKR2_HUMAN</i>	Kruppel-related zinc finger protein 2 (Protein HKR2) (Zinc finger protein 50) (Zinc finger and SCAN domain-containing protein 22) (Fragment) [Source: Uniprot/SwissProt:Acc:P10073]	10	1	-3.32
<i>HIVEP3</i>	[Source:RefSeq_peptide:Acc:NP_076770] [Source: Uniprot/SwissProt:Acc:P10073]	19	2	-3.25
<i>GPCR35</i>	Probable G-protein coupled receptor 35 [Source: Uniprot/SwissProt:Acc:Q9HC97]	19	2	-3.25
<i>C1orf145</i>	C1orf145 protein (Fragment) [Source: Uniprot/SPTREMBL:Acc:Q8N372]	19	2	-3.25
<i>CBX6</i>	Chromobox protein homolog 6 [Source: Uniprot/SwissProt:Acc:Q95503]	28	3	-3.22
<i>Q9H353_HUMAN</i>	-	37	4	-3.21
<i>C11orf69</i>	Uncharacterized protein C11orf69 [Source: Uniprot/SwissProt:Acc:Q8QY44]	37	4	-3.21
<i>MYF5</i>	Myogenic factor 5 (Myf-5) [Source: Uniprot/SwissProt:Acc:P13349]	9	1	-3.17
<i>PRKAR2B</i>	[Source: Uniprot/SwissProt:Acc:P13323]	9	1	-3.17
<i>NOX1</i>	NADPH oxidase homolog 1 (NOX-1) (NOH-1) (NADH/NADPH oxidase subunit P65-MOX) (Mitogenic oxidase 1) (MOX1) [Source: Uniprot/SwissProt:Acc:Q9Y558]	9	1	-3.17
<i>ELOVL3</i>	Elongation of very long chain fatty acids protein 3 (Cold-inducible glycoprotein of 30 kDa) [Source: Uniprot/SwissProt:Acc:Q9H803]	45	5	-3.17
<i>BCL2L10</i>	Apoptosis regulator Bcl-2 (Bcl-2-like 10 protein) (Bcl2-L-10) (Anti-apoptotic protein NrH) [Source: Uniprot/SwissProt:Acc:Q9HD36]	18	2	-3.17
<i>SEPT8</i>	Septin-8 [Source: Uniprot/SwissProt:Acc:Q92599]	18	2	-3.17
<i>C17orf57</i>	C17orf57 protein [Source: Uniprot/SPTREMBL:Acc:Q9A9G9]	18	2	-3.17
<i>SPANX2</i>	SPANX-2 protein [Source: RefSeq_peptide:Acc:NP_001009615]	9	1	-3.17
<i>CHST3</i>	(GlcNAc6S-T-3) (Intestinal GlcNAc-6-sulfotransferase) (Intestinal N-acetylglucosamine-6-O-sulfotransferase) (GlcNAc6ST) (hGlc6ST) (Galactose/N-acetylglucosamine [Source: Uniprot/SwissProt:Acc:Q9GZ59]	26	3	-3.12
<i>DLI0X2A</i>	[Source: Uniprot/SwissProt:Acc:Q1HG44]	26	3	-3.12
<i>FAM26A</i>	Protein FAM26A [Source: Uniprot/SwissProt:Acc:Q86XJ0]	69	8	-3.11
<i>NEURL2</i>	Neuralized-like protein 2 [Source: Uniprot/SwissProt:Acc:Q9BR09]	43	5	-3.1
<i>TERT</i>	Telomerase reverse transcriptase (EC: 2.7.7.49) (Telomerase catalytic subunit) (HEST2) (Telomerase-associated protein 2) (TP2) [Source: Uniprot/SwissProt:Acc:G14746]	34	4	-3.09
<i>MDU64</i>	NADH dehydrogenase [ubiquinone] alpha subcomplex subunit 4 (EC: 1.6.3.3) (EC: 1.6.99.3) (NADH:ubiquinone oxidoreductase MLRQ subunit) (Complex I-MLRQ) (CI-MLRQ) [Source: Uniprot/SwissProt:Acc:Q00831]	4846	593	-3.08
<i>ART1</i>	GPI-linked NAD(P)+-arginine ADP-ribosyltransferase 1 precursor (EC: 2.4.2.31) (Mono(ADP-ribose)yltransferase) (CD296 antigen) [Source: Uniprot/SwissProt:Acc:P52961]	8	1	-3
<i>NP_001001684.1</i>	CDNA FLJ48831 fs, clone NT2R96007416 [Source: Uniprot/SPTREMBL:Acc:Q6Z549]	8	1	-3
<i>AKAP3</i>	A-kinase anchor protein 3 (Protein kinase A-anchoring protein 3) (PKA3) (A-kinase anchor protein 110 kDa) (AKAP110) (Sperm oocyte-binding protein) (Fibrous sheath 1) (Fibrous sheath protein of 95 kDa) (FSP95) [Source: Uniprot/SwissProt:Acc:Q75966]	8	1	-3
<i>GTTF2IRD2</i>	GTTF2 repeat domain containing 2 [Source: RefSeq_peptide:Acc:NP_778808]	8	1	-3
<i>SPATA16</i>	spermatogenesis associated 16 [Source: RefSeq_peptide:Acc:NP_114161]	23	3	-2.94
<i>SPIN1LW1</i>	Eppin precursor (Epitidymal protease inhibitor) (Serine protease inhibitor-like with Kunitz and WAP domains 1) (WAP four-disulfide core domain protein 7) (Protease inhibitor WAP7) [Source: Uniprot/SwissProt:Acc:Q95925]	23	3	-2.94
<i>OR2L2</i>	Olfactory receptor 2L2 (HTRCRH07) [Source: Uniprot/SwissProt:Acc:Q8NH16]	23	3	-2.94
<i>HTR5A</i>	5-hydroxytryptamine 5A receptor (5-HT-5A) (Serotonin receptor 5A) (5-HT-5) [Source: Uniprot/SwissProt:Acc:P47898]	30	4	-2.91
<i>CFI05_HUMAN</i>	[Source: Uniprot/SwissProt:Acc:Q6UAX7]	30	4	-2.91
<i>Q9H7Y2_HUMAN</i>	CDNA FLJ14100 fs, clone MAMMA1000855 [Source: Uniprot/SPTREMBL:Acc:Q9H7Y2]	30	4	-2.91
<i>ZP42</i>	zinc finger protein 42 [Source: RefSeq_peptide:Acc:NP_777560]	15	2	-2.91
<i>C1orf112</i>	C1orf112 protein [Source: Uniprot/SPTREMBL:Acc:Q3KNQ1]	15	2	-2.91
<i>EDAR</i>	Tumor necrosis factor receptor superfamily member EDAR precursor (Anhidrotic ectodysplasin receptor 1) (Ectodysplasin-A receptor) (EDA-A) receptor (Ectodermal dysplasia receptor) (Downless homolog) [Source: Uniprot/SwissProt:Acc:Q9J9H1]	15	2	-2.91
<i>RNF11</i>	RING finger protein 11 (Ssd 1669) [Source: Uniprot/SwissProt:Acc:Q9Y3C5]	949	129	-2.88
<i>CLDN14</i>	Claudin-14 [Source: Uniprot/SwissProt:Acc:Q95500]	22	3	-2.87
<i>SGCZ</i>	Zeta-sarcoglycan (Zeta-SG) (ZSG1) [Source: Uniprot/SwissProt:Acc:Q96L11]	29	4	-2.86
<i>PLAC8</i>	Placenta-specific gene 8 protein (Protein C15) [Source: Uniprot/SwissProt:Acc:Q9NZF1]	121	17	-2.83
<i>LRRC17</i>	[Source: Uniprot/SwissProt:Acc:Q8N6Y2]	7	1	-2.81
<i>PCDH7</i>	[Source: Uniprot/SwissProt:Acc:Q60245]	35	5	-2.81
<i>TRAV22</i>	T-cell receptor alpha V gene segment [Source: IMG/GENE:DB:Acc:TRAV22]	7	1	-2.81
<i>XAB2</i>	XPA-binding protein 2 (XCN2) protein [Source: Uniprot/SwissProt:Acc:Q9HC37]	35	5	-2.81
<i>FCGR2A</i>	(IgG Fc receptor 1a) (F-gamma-R1a) (CD32 antigen) (C1w32) [Source: Uniprot/SwissProt:Acc:P12318]	21	3	-2.81
<i>SEC14L5</i>	-	21	3	-2.81
<i>C11orf53</i>	Uncharacterized protein C11orf53 [Source: Uniprot/SwissProt:Acc:Q8N6V4]	21	3	-2.81
<i>LOC729516</i>	-	21	3	-2.81
<i>SLFN1</i>	schlafen-like 1 [Source: RefSeq_peptide:Acc:NP_659427]	14	2	-2.81

Gene Symbol	Description	ncRNA	miR-210	Log(ratio)
<i>LRAT</i>	Lecithin retinoyl acyltransferase (EC 2.3.1.135) (Phosphatidylcholine--retinoyl O-acyltransferase). [Source:Uniprot/SWISSPROT;Acc:Q95237]	7	1	-2.81
<i>GPR177</i>	Integral membrane protein GPR177 precursor (Protein without homolog) (Putative NF-kB-activating protein-37). [Source:Uniprot/SWISSPROT;Acc:Q5796_2]	817	121	-2.76
<i>ADAMTS13</i>	ADAMTS13 precursor (EC 3.4.24.1) (A disintegrin and metalloproteinase with thrombospondin motifs 13) (ADAM-TS13) (ADAM-TS13) (von Willebrand factor-cleaving protease) (vWF-CP). [Source:Uniprot/SWISSPROT;Acc:Q76_XS1]	47	7	-2.75
<i>PTCH1D1</i>	patched domain containing 1 [Source:RefSeq;peptide;Acc:NP_775766]	20	3	-2.74
<i>ACPL2</i>	acid phosphatase-like 2 [Source:RefSeq;peptide;Acc:NP_001032249]	20	3	-2.74
<i>TTEC</i>	transcription factor EC isoform B [Source:RefSeq;peptide;Acc:NP_001018068]	33	5	-2.72
	phosphoprotein p18 (P17) (Proslin) (Metablastin) (Protein P22). [Source:Uniprot/SWISSPROT;Acc:P16949]	1003	153	-2.71
<i>Q8WYR5_HUMAN</i>	Tumor rejection antigen [Source:Uniprot/SPTREMBL;Acc:Q8WYR5]	557	85	-2.71
<i>Q8NH10</i>	MGC32805 protein. [Source:Uniprot/SPTREMBL;Acc:Q8NH10]	26	4	-2.7
<i>C7orf39</i>	UFP0388 protein C2orf39. [Source:Uniprot/SWISSPROT;Acc:Q9H7X2]	26	4	-2.7
	Pregnancy-specific beta-1-glycoprotein 10 precursor (PSBG-10) (PSBG-12). [Source:Uniprot/SWISSPROT;Acc:Q15235]	13	2	-2.7
<i>PSG10</i>	Gap junction alpha-5 protein (Connexin-40) (Cx40). [Source:Uniprot/SWISSPROT;Acc:P36382]	13	2	-2.7
<i>POT15_HUMAN</i>	[Source:Uniprot/SWISSPROT;Acc:Q655H4]	13	2	-2.7
<i>NP_001008784.1</i>	CD200 cell surface glycoprotein receptor isoform 2 [Source:RefSeq;peptide;Acc:NP_001008784]	13	2	-2.7
	Period circadian protein homolog 3 (Circadian clock protein PERIOD 3) (hPER3). [Source:Uniprot/SWISSPROT;Acc:P56645]	45	7	-2.68
<i>PER3</i>	putative membrane protein HEP [Source:RefSeq;peptide;Acc:NP_741997]	44	7	-2.65
<i>TEDDM1</i>	Dedicator of cytokinesis protein 4. [Source:Uniprot/SWISSPROT;Acc:Q8N110]	25	4	-2.64
<i>DOCK4</i>	Regulating synaptic membrane exocytosis protein 3 (Nim3) (Rab-3-interacting molecule 3) (RIM3) (RIM3 gamma). [Source:Uniprot/SWISSPROT;Acc:Q91J10]	43	7	-2.62
<i>RIMS3</i>	Fc receptor-like 3 precursor [Source:RefSeq;peptide;Acc:NP_443171]	49	8	-2.61
<i>ICRL3</i>	Glucocorticoid regulatory protein (Glucocorticoid regulator). [Source:Uniprot/SWISSPROT;Acc:Q14397]	6	1	-2.58
<i>GCCR</i>	Na ⁺ /H ⁺ exchanger like domain containing [Source:RefSeq;peptide;Acc:NP_631912]	24	4	-2.58
<i>NP_631912.2</i>	CDNA FLJ25369 fs, clone TS101830 (Hypothetical protein FLJ25369) (Chromosome 2 open reading frame 51). [Source:Uniprot/SPTREMBL;Acc:Q961M6]	48	8	-2.58
<i>C2orf51</i>	Homeobox protein engrailed-2 (Hs-Ea-2). [Source:Uniprot/SWISSPROT;Acc:P19622]	30	5	-2.58
<i>EN2</i>	Ret finger protein-like 1 (RING finger protein 78). [Source:Uniprot/SWISSPROT;Acc:Q78677]	30	5	-2.58
<i>RFP1L</i>	Growth differentiation factor 3 precursor (GDF-3). [Source:Uniprot/SWISSPROT;Acc:Q9NR23]	36	6	-2.58
<i>GDF3</i>	CDNA FLJ37357 fs, clone BRAMY2023066 (FLJ37357 protein) (Hypothetical protein FLJ37357). [Source:Uniprot/SPTREMBL;Acc:Q8N1W6]	30	5	-2.58
<i>NP_775916.1</i>	Intestine-specific homeobox [Source:RefSeq;peptide;Acc:NP_001008494]	24	4	-2.58
<i>ISX</i>	CX3C chemokine receptor 1 (CX3C-CR1) (CXCR1) (F-metakinin receptor) (G-protein coupled receptor 13) (V28) (Beta chemokine receptor-like 1) (CMK-BRL-1) (CMKBLR1). [Source:Uniprot/SWISSPROT;Acc:P49238]	24	4	-2.58
<i>CX3CR1</i>	Melanoma inhibitory activity protein 2 precursor. [Source:Uniprot/SWISSPROT;Acc:Q96FC5]	18	3	-2.58
<i>MIA2</i>	Olfactory receptor 10D4. [Source:Uniprot/SWISSPROT;Acc:Q8NGN7]	18	3	-2.58
<i>O10D4_HUMAN</i>	Olfactory receptor 7G2 (Olfactory receptor 19-13) (OR19-13) (OST260). [Source:Uniprot/SWISSPROT;Acc:Q8C991]	18	3	-2.58
<i>OR7G2</i>	Low-density lipoprotein receptor-related protein 2 precursor (Megalyn) (Glycoprotein 330) (gp330). [Source:Uniprot/SWISSPROT;Acc:P98164]	12	2	-2.58
<i>LRP2</i>	Putative uncharacterized protein C2orf46. [Source:Uniprot/SWISSPROT;Acc:Q6ZSR3]	12	2	-2.58
<i>C2orf46</i>	[Source:Uniprot/SPTREMBL;Acc:Q6ZM19]	6	1	-2.58
<i>Q6ZM19_HUMAN</i>	Complement C1q tumor necrosis factor-related protein 2 precursor. [Source:Uniprot/SWISSPROT;Acc:Q9BXL5]	6	1	-2.58
<i>C1QTNF2</i>	Serine hydrolase-like protein 2 (EC 3.1.-.-). [Source:Uniprot/SWISSPROT;Acc:Q9H4I8]	64	11	-2.54
<i>SERHL2</i>	USH1C-binding protein 1 (Usher syndrome type-1C protein-binding protein 1) (MCC-2) (AIE-75-binding protein). [Source:Uniprot/SWISSPROT;Acc:Q8M6V0]	29	5	-2.54
<i>USH1P1</i>	[Source:Uniprot/SWISSPROT;Acc:Q8T4G5]	23	4	-2.53
<i>U8TMD1</i>	sulfate proteoglycan core protein 1 [Contains: Aggrecan core protein 2]. [Source:Uniprot/SWISSPROT;Acc:P16112]	23	4	-2.52
<i>AGC1</i>	[Source:Uniprot/SWISSPROT;Acc:Q14599]	23	4	-2.52
<i>BPY2C</i>	Dolichyl 4-phosphoglycosaccharide--protein glycosyltransferase 48 kDa subunit precursor (EC 2.4.1.119) (Oligosaccharyl transferase 48 kDa subunit) (DDOST 48 kDa subunit). [Source:Uniprot/SWISSPROT;Acc:P39656]	2238	391	-2.52
<i>DDOST</i>	Iroquois-class homeodomain protein IRX-1 (Iroquois homeobox protein 1) (Homeodomain protein IRX1). [Source:Uniprot/SWISSPROT;Acc:P78414]	34	6	-2.5
<i>IRX1</i>	T-cell surface glycoprotein CD4 precursor (T-cell surface antigen T4L.eu-3). [Source:Uniprot/SWISSPROT;Acc:P01730]	17	3	-2.5
<i>CD4</i>	CDNA FLJ35343 fs, clone PROST2015932. [Source:Uniprot/SPTREMBL;Acc:Q8NAH5]	17	3	-2.5
<i>Q8NAH5_HUMAN</i>	Pregnancy-specific beta-1-glycoprotein 2 precursor (PSBP2) (Pregnancy-specific beta-1 glycoprotein E) (PS-beta-E). [Source:Uniprot/SWISSPROT;Acc:P11465]	28	5	-2.49
<i>PSG2</i>	Thrombospondin-1 precursor. [Source:Uniprot/SWISSPROT;Acc:P07996]	206	37	-2.48
<i>THBS1</i>	Ankyrin repeat domain-containing protein 20A3. [Source:Uniprot/SWISSPROT;Acc:Q5VUR7]	22	4	-2.46
<i>ANKRD20A3</i>				

Gene Symbol	description	ncRNA	miR-210	Log2(ratio)
FNBP1L	Formin-binding protein 1-like (Transducer of Cdc42-dependent actin assembly protein 1) (Toca-1). [Source:Uniprot/SWISSPROT:Acc:Q5TON5]	33	6	-2.46
HBB	Hemoglobin subunit beta (Hemoglobin beta chain) (Beta-globin). [Source:Uniprot/SWISSPROT:Acc:P88711]	22	4	-2.46
WIP1L3	Pw1-like protein 3. [Source:Uniprot/SWISSPROT:Acc:Q723Z3]	22	4	-2.46
MAGEA11	Melanoma-associated antigen 11 (MAGE-11 antigen). [Source:Uniprot/SWISSPROT:Acc:P43364]	22	4	-2.46
KCNJ1	Potassium voltage-gated channel subfamily G member 1 (Voltage-gated potassium channel subunit Kv6.1) (4FD). [Source:Uniprot/SWISSPROT:Acc:Q9L1X4]	11	2	-2.46
ADRA1A	Alpha 1A adrenergic receptor (Alpha 1A-adrenoceptor) (Alpha-1C ⁺ adrenergic receptor (Alpha adrenergic receptor 1c). [Source:Uniprot/SWISSPROT:Acc:P35348]	11	2	-2.46
NP_001001343.1	MGIC27121 gene (MGIC27121). mRNA [Source:RefSeq_dna:Acc:NM_001001343]	38	7	-2.44
GFNMB	Transmembrane glycoprotein NMB precursor (Transmembrane glycoprotein HGFIN). [Source:Uniprot/SWISSPROT:Acc:Q14956]	54	10	-2.43
C1orf173	C1orf173 protein. [Source:Uniprot/SPTREMBL:Acc:Q6GM88]	27	5	-2.43
NTS	Neurotensin/neurotensin N precursor [Contains: Large neurotensin N (NmN-125); Neurotensin N (NmN) (NN); Neurotensin (NT); Tail peptide]. [Source:Uniprot/SWISSPROT:Acc:P30990]	27	5	-2.43
XKR4	XK-related protein 4. [Source:Uniprot/SWISSPROT:Acc:Q5GH76]	16	3	-2.42
C12orf59	C12orf59 protein. [Source:Uniprot/SPTREMBL:Acc:Q4KMG9]	159	30	-2.41
USP29	specific-processing protease 29 (Deubiquitinating enzyme 29). [Source:Uniprot/SWISSPROT:Acc:Q9HB17]	21	4	-2.39
PLA2G7	acylhydrolase (LDL-associated phospholipase A2) (LDL-PLA(2)) (2-acetyl-1-alkylglycerophosphocholine esterase) (1-alkyl-2-acetyl-glycerophosphocholine esterase) [Source:Uniprot/SWISSPROT:Acc:Q13093]	21	4	-2.39
NP_001006565.1	MSTP119. [Source:Uniprot/SPTREMBL:Acc:Q722S5]	21	4	-2.39
CEFCAM1	cerebral endothelial cell adhesion molecule 1 [Source:RefSeq_peptide:Acc:NP_057258]	21	4	-2.39
ZDHHC22	Putative palmitoyltransferase ZDHHC22 (EC 2.3.1.-) (Zinc finger DHHC domain-containing protein 22) (DHHC-22). [Source:Uniprot/SWISSPROT:Acc:Q8N966]	21	4	-2.39
ZNF101	Zinc finger protein 101 (Zinc finger protein HFZ12). [Source:Uniprot/SWISSPROT:Acc:Q81ZC7]	47	9	-2.38
ADRA1B	Alpha 1B adrenergic receptor (Alpha 1B-adrenoceptor) (Alpha 1B- adrenoceptor). [Source:Uniprot/SWISSPROT:Acc:P35368]	26	5	-2.38
ACOX3	Acyl-coenzyme A oxidase 3, peroxisomal (EC 1.3.3.6) (Pristanoyl-CoA oxidase) (Branched-chain acyl-CoA oxidase) (BRC ACox). [Source:Uniprot/SWISSPROT:Acc:Q15254]	31	6	-2.37
Q8N750_HUMAN	CDNA FLJ40244 fs. clone TEST12039026. [Source:Uniprot/SPTREMBL:Acc:Q8N750]	31	6	-2.37
PHKG1	Phosphorylase b kinase gamma catalytic chain, skeletal muscle isoform (EC 2.7.1.19) (Phosphorylase kinase subunit gamma 1). [Source:Uniprot/SWISSPROT:Acc:Q16816]	31	6	-2.37
LRP5L	low density lipoprotein receptor-related protein 5-like [Source:RefSeq_peptide:Acc:NP_872298]	67	13	-2.37
AAK1	AP2-associated protein kinase 1 (EC 2.7.11.1) (Adaptor-associated kinase 1). [Source:Uniprot/SWISSPROT:Acc:Q2M1B9]	221	43	-2.36
KIAA0195	KIAA0195 (KIAA0195). mRNA [Source:RefSeq_dna:Acc:NM_014738]	40	8	-2.32
Q8NA59_HUMAN	CDNA FLJ35816 fs. clone TEST12006109. [Source:Uniprot/SPTREMBL:Acc:Q8NA59]	30	6	-2.32
EMID1	EMI domain-containing protein 1 precursor (Protein Emi1) (Emi1 and multimerin domain-containing protein 1). [Source:Uniprot/SWISSPROT:Acc:Q96A84]	5	1	-2.32
C6orf122	Uncharacterized protein C6orf122. [Source:Uniprot/SWISSPROT:Acc:Q5T6M2]	20	4	-2.32
ERC1	ELKS/RAB6-interacting/CAST family member 1 (RAB6-interacting protein 2) (ERC protein 1). [Source:Uniprot/SWISSPROT:Acc:Q8LIJ2]	20	4	-2.32
USP6	Ubiquitin carboxyl-terminal hydrolase 6 (EC 3.1.2.15) (Ubiquitin thioesterase 6) (Ubiquitin-specific-processing protease 6) (Deubiquitinating enzyme 6) (Proto-oncogene TRE-2). [Source:Uniprot/SWISSPROT:Acc:P35125]	20	4	-2.32
GRB14	Growth factor receptor-bound protein 14 (GRB14 adapter protein). [Source:Uniprot/SWISSPROT:Acc:Q14449]	15	3	-2.32
ALG10	(Asparagine-linked glycosylation protein 10 homolog A). [Source:Uniprot/SWISSPROT:Acc:Q5BK14]	15	3	-2.32
SPTB	Spectrin beta chain, erythrocyte (Beta-1 spectrin). [Source:Uniprot/SWISSPROT:Acc:P11277]	10	2	-2.32
C3AR1	[Source:Uniprot/SWISSPROT:Acc:Q16581]	10	2	-2.32
HTR2C	5-hydroxytryptamine 2C receptor (5-HT-2C) (Serotonin receptor 2C) (5-HT2C) (5-HT2C) (5HT-1C). [Source:Uniprot/SWISSPROT:Acc:Q29K35]	10	2	-2.32
O65724_HUMAN	Reverse transcriptase (Fragment). [Source:Uniprot/SPTREMBL:Acc:O95724]	5	1	-2.32

The fifteen genes predicted as a miR-210 target gene by microCosm, TargetScan or PicTar were highlighted in gray.

Supplementary Table 3. The list represents 811 genes predicted as a miR-210 target gene by microCosm, TargetScan and PicTar

ABC1	C10orf122	C8A	EFNA3	G12	JMP3
ABC9P2	C11orf2	CD99	EGFL9	G1A7	IQCC
ABCD1	C11orf8	CDCL1	CDL3	GL1	IQCC
ABCD4	C11orf59	CDCL2	EGR4	GLJ1	IRX6
ABHD2	C11orf63	CDH26	EHD2	GLS2	ISCA2
AB12	C12orf34	CDH1C	EIF359	GNA15	ISCU
ABTB1	C12orf48	CDX2	ELF2	GNA17	ITGA5
AC006273.1	C14orf148	CEND1	ELAC2	GN33	ITGB4
AC008772.1	C15orf43	CETN3	ELFN2	GNG8	IWS1
AC008989.1	C15orf52	CHFR2	ELOVL6	GOLGA1	IOSD2
AC009967.5	C15orf62	CHAD	EMID1	GOLGA2LY	KALG1
AC02016.6	C16orf35	CHD1L	EMI2	GOLPH3	KCNM1
AC040977.2	C16orf70	CHEK2	ENP22	GPDI1L	KCNH5
AC109322.1	C17orf57	CHES1	ENSA	GPR153	KCNMB1
AC114488.5	C17orf84	CHN1	EPH4L1	GPR17	KCNQ2
AC133485.1	C17orf83	CHRD1L	EPGN	GPR177	KCNQ2
AC141586.2	C18orf10	CHRM3	EPHA2	GPR19	KIAA0664
AC226119.1	C18orf34	CHRM1	EPHB2	GPR39	KIAA0748
ACP1	C19orf16	CHRMG	EPH5	GPR87	KIAA1622
ACTA1	C19orf34	CHST1	ERF27	GRIA2	KIAA1751
ACTC1	C19orf59	CHST2	EVL	GRIK2	KIAA1755
ACTG1	C19orf102	CHUK	EVPL	GRIN3B	KIAA2013
ACTL7A	C19orf110	CHRB	EXOSC10	GRIN1A	KIF13B
ADA	C19orf111	CLDN15	F11R	GRM5	KIF20A
ADAMTS7	C19orf112	CLEC11A	F7	GRM6	KIR2DL1
ADCY7	C19orf116	CLEC19A	FAMH3	GSC	KLHDC4
AGW12	C19orf128	CNME1	FAM105B	GSTA1	KLH15
AGTRAP	C19orf133	COL1A1	FAM108A1	GSTA2	KLRA1
AGTRL1	C19orf167	COLA2	FAM108A2	GSTT2	KLR4
AGXT2L2	C19orf184	COL4A3	FAM116A	GZT21	KRATP5-4
AHR	C19orf206	COL4A2	FAM120A	LAR2	KRATP5-4
AFM3	C19orf88	COL5A3	FAM12A	HAO	LAMA3
AKAP7	C1QTNF4	COMMD4	FAM149A	HAS1	LAMA5
AKAP9	C1S	COX10	FAM25A	IKC4	LAMC3
AKRIC12	C20orf103	CPNE2	FAM25B	HDLBP	LMBP1
AL132661.1	C20orf195	CR1	FAM25C	HEATR2B2	LCK
AL161662.2	C2orf32	CREBB3L3	FAM5B	HELZ	LDNB
ALDH1A1	C2orf46	CRHBP	FAM73B	HHP	LDHB
ALDH1A1	C3orf21	CRF1	FAM8A	HFA3	LEAP2
ALKBK3	C3orf30	CRVB4	FAM90A1	HHRF3	LG3
ALC	C4orf23	CS	FAM90A10	HIST1H1B	LHP
AMBN	C6orf125	CSPP1	FAM90A18	HIST1H2AK	LJPE
ANAPC7	C6orf145	CSY3	FAM90A3	H3	LJI
ANK1	C6orf184	CTBP2	FAM90A7	HLYB9	LMAN1L
ANKRD24	C6orf191	CUEDC2	FAM90A8	HMG20B	LMTK2
ANKRD41	C6orf57	CUL9	FAM90A9	HMOX3	LMB1B
ANKK3	C9	CYBR2	FAM9B	HPCA	LOC399947
AP000355.2	C9orf129	CYGB	FANCB	HPCAL1	LOC643224
AP000689.1	C9orf134	CYP11B1	FANCE	HRH2	LRFN1
AP0BIC3G	C9orf78	CYP2F1	FANF1	HSD17B1	LRF5L
ARFP1	C9orf85	DAB1	FBX12	HSD17B7	LRP4P1
ARHGAP17	C9orf86	CNAR1	FBX16	HSP48	LRR62
ARHGFE17	C9orf93	DBN1	FBX17	HSPBAP1	LRR68
ARMC1	CACNA2D2	DCHS1	FBXW5	HSTAF51	LRRCA8
ARMC4	CALCCO1	DCY7L	FER1L4	HTRAI	LRRCS0
ARSD	CAMK2G	DDX24	FEZF1	HVAL1	LRRCS0
ASCC1	CAPN10	DDX51	FGD1	ID2	LRSAM1
ASCL1	CAPN9	DEAF1	FGF10	IGF1R	LYOH
ASL	CARD9	DECI	FGF18	IGHA2	LYN
ATGD4	CASQ1	DEFB118	FGF22	IGHV3-13	LYPLA2
ATN1	CCBP2	DGKA	FGFR1	IGHV3-16	MAG2
ATP12A	CCDC46	DGKG	FH1T	IGHV3-23	MAN1B1
ATP1B1	CCDC17	DHRS3	FHOD1	IGHV3-35	MAR6
ATP2B3	CCDC24	DHXS8	FHPL4	IGHV3-38	MARPD1
ATP6V9C	CCDC28A	DMT1L	FMO1	IGHV3-47	MORC14
AVP	CCDC28B	DNAH11	FNTA	IGHV3-66	MARR1
AVP1B	CCDC53	DNAEC16	FOND2	IKR34	MAST1
BGAL15	CCDC85	DNAEC4	FONL3	IGL4	MBO5
B4GAL15	CCDC97	DNAJC8	FRAP1	IGLL3	MCCD1
B4GAL17	CCKBR	DPEP2	FRY	IGSF21	MCM4
BAP3	CCNB1P1	DPS15	FTSJ2	IFPK2	MGMR
BCA2	CCND2	DNS2	FTN3	IFPK3	MDGA1
BCL2L12	CCT3	DTX1	G0S2	IKBK1	MEF2D
BDNF	CD180	DUOX1A1	GAK	IL1RA	MEGF6
BICD1	CD22	DUSP12	GARNL1	IL17RC	MEIS1
BR144L	CD276	DUSP28	GAS6	IL18	MEIS4P3
BTBD10	CD300LD	E2F3	GBG1	IL3RA	MFS14
BX12478.1	CD55	EBF3	GDAP1L1	ILVBL	MI11P1

Supplementary Table 3. The list represents 811 genes predicted as a miR-210 target gene by microCosm, TargetScan and PicTar

MINA	PCP4	RP4-365E6.J	SURF5	WNT9B
MLL2	PCSK7	RP52	SUSD1	XCR1
MPV17L	PHF15	RSC1A1	SUZ12	XRR5
MRPL36	PDE3A	RUFY1	SYNE2	XRRAI
MRP530	PDLIM3	RUVBL2	SYNGAP1	YIPF3
MS4A8B	PDX1	SACMHL	SYT15	YY1
MT4	PDD2D4	SAMDJ3	TAC4	Z97R0.2
MUC4	PEX10	SAP9L	TAP6	ZBTB12
MX1	PEX13	SARNP	TBC1D16	ZCCHC11
MXD4	PEX5L	SCGB1C1	TBC1D28	ZDHHC12
MTH1	PHF15	SCN1B	TBC1D8	ZDHHC4
MYO15B	PHF23	SCN9A	TCF7L2	ZFPM1
MYOHD1	PHKG2	SCOC	TCHP	ZHX2
MYT1L	PHF11	SCRT1	TFAP2A	ZMAT4
NAT14	PHKAP2	SCTE1	TFCP2	ZME2
NDUFA4	PIK3R5	SDCCAG8	TGFBRAP1	ZMYM2
NEFM	PIK4CA	SDF2	THOC5	ZMYM6
NEK1	PKNOX2	SDHALP1	TIAM1	ZNF227
NEUROD2	PLA1A	SDHALP2	TGID2	ZNF274
NEUROG3	PLCB3	SEC24C	1IGD5	ZNF397
NFIB	PLCD3	SEH1L	TIMM17B	ZNF403
NFIL3	PLK1	SENP8	TIMP1	ZNF418
NKX2-5	PLNKC1	SEPT12	TLX1	ZNF435
NKX2-8	PODN	SERPINA12	TMEM142A	ZNF462
NOMO1	POF1B	SERPINA3	TMEM16B	ZNF467
NOMO3	POLR21	SETD2	TMEM16D	ZNF583
NOX4	POL2AF1	SF3B1	TMEM194B	ZNF585B
NP_660343.1	NP_660343.1	SF3B4	TMEM195	ZNF720
NP_683701.2	NP_683701.2	SF3B5	TMEM204	ZNF827
NPHP4	PPP1CC	SH2D7	TMEM208	ZRANB3
NPM3	PPP1R12C	SH3BGR	TMEM40	ZSCAN20
NPR1	PPP1R16A	SH3BGL	TNFRSF13C	
NPSR1	PPP3R1	SH3KBP1	TNPI1	
NPTX1	PRHOXNB	SHC3	TNIP3	
NQO2	PRICKLE4	SHCBP1	TNPO3	
NR6A1	PRKAA1	SID2	TOM1L2	
NRG4	PRMT2	SILI	TOR1A	
NRGN	PRPF38B	SIN3B	TP53TG3	
NSDHL	PRR1	SIPA1L3	TPST1	
NSUN5	PRKG2	SIX1	TRAPD1	
NTSC1B	PRSSI6	SLC12A8	TRAV4	
NTSDC1	PSG2	SLC15A1	TRIM4	
NTN4	PSME3	SLC16A14	TRIM17	
NUDT6	PTAFR	SLC20A1	TSEN2	
NUP133	PTCHD3	SLC25A28	TSNAXIP1	
NUP12	PTGES2	SLC26A3	TSPAN10	
NUPR1	PTS	SLC2A1	TSPAN4	
NTX	PTDC1	SLC37A1	TTC12	
OAF	PYV	SLC38A5	TTC13	
OBSCN	Q6ZRP6_HUMAN	SLC43A1	TTC24	
ODF3	Q9BZU2_HUMAN	SLC4A11	TTC4	
ODZ2	Q9UBB8_HUMAN	SLC6A19	TTI1	
ODZ3	RAB26	SLITRK5	TLL1	
OGG1	RAB27B	SMARCA4	TXNL6	
OLFML2A	RAB6AP1L	SMCHD1	UBASH3A	
OLIG3	RALG2	SOXBS2	UBE2E	
OR10G8	RALGDS	SOX21	UBN2	
OR2T8	RANBP5	SOX30	UBQLN1	
OR2V2	RASSAL2	SOPCA3	UMODL1	
OR6A14	RASSF1	SPKCA4	UNC5A	
OR4P1P	RASSF6	SPO11	UNC5A	
OR5M13P	RBM3	SPRR2F	URM1	
OSBP2L	RBM11C	SPTB	URSD	
OTOS	RBPPL	SQLE	USP21	
OTP	RC3H1	SREBF1	USP6NL	
OTUB1	RECK	SRMS	VIT	
P2RX1	RETN	SRPX	VKRI	
P2RY10	RGM1TD1	STK3AL3	VXOG6	
P2RY11	RG5A	STGALNAC6	VWASB1	
P4HA3	RIBC2	STAB1	WDFY2	
PABPC1L	RLN3	STARBDNL	WDR20	
PADI1	RNF107	STAF6	WDR22	
PANX3	RNF208	STIP1	WDR38	
PAOX	RNF212	STT3B	WDR5B	
PARR2	RP1-163G9.1	STX11	WDR6	
PBX1	RP1-181G12.1	STX1R2	WDR64	
PCBP4	RP11-191L9.1	STXBP5	WDR66	
PCHD21	RP11-397P14.1	SUMO3	WISP2	



ORIGINAL ARTICLE

MicroRNA-141 confers resistance to cisplatin-induced apoptosis by targeting *YAP1* in human esophageal squamous cell carcinoma

Yukako Imanaka¹, Soken Tsuchiya², Fumiaki Sato², Yutaka Shimada³, Kazuharu Shimizu² and Gozho Tsujimoto¹

MicroRNAs (miRNAs) are endogenous non-coding RNAs that function as negative regulators of gene expression. Alterations in miRNA expression have been shown to affect tumor growth and response to chemotherapy. In this study, we explored the possible role of miRNAs in cisplatin resistance in esophageal squamous cell carcinoma (ESCC). First we assessed the sensitivity of nine human ESCC cell lines (KYSE series) to cisplatin using an *in vitro* cell viability assay, and then we compared the miRNA profiles of the cisplatin-sensitive and -resistant cell lines by miRNA microarray analysis. The two groups showed markedly different miRNA expression profiles, and 10 miRNAs were found to be regulated differentially between the two groups. When miR-141, which was the most highly expressed miRNA in the cisplatin-resistant cell lines, was expressed ectopically in the cisplatin-sensitive cell lines, cell viability after cisplatin treatment was increased significantly. Furthermore, we found that miR-141 directly targeted the 3'-untranslated region of *YAP1*, which is known to have a crucial role in apoptosis induced by DNA-damaging agents, and thus downregulated *YAP1* expression. Our study highlights an important regulatory role for miR-141 in the development of cisplatin resistance in ESCC.

Journal of Human Genetics advance online publication, 3 February 2011; doi:10.1038/jhg.2011.1

Keywords: apoptosis; cisplatin resistance; esophageal carcinoma; microRNA; *YAP1*

INTRODUCTION

MicroRNAs (miRNAs) are a class of small (~ 22 bp) endogenous non-coding RNAs that are well conserved, and function as negative regulators of gene expression. miRNAs bind to complementary sequences in the 3'-untranslated region (UTR) of target messenger RNAs and regulate their expression by cleavage and/or translational inhibition.¹ miRNAs are predicted to regulate the expression of up to one-third of human protein-coding genes,^{2–5} and they have been shown to have crucial roles in diverse biological processes, including development, differentiation, apoptosis and proliferation.^{6–8} A growing number of studies have provided strong evidence that aberrant miRNA expression is involved in the genesis and progression of cancer,⁹ and that miRNAs might function as a novel class of oncogenes or tumor-suppressor genes.^{10–13} Altered expression of miRNAs in primary human cancers has been used for tumor diagnosis, classification, staging and prognosis.¹⁴ Furthermore, the involvement of miRNAs in the response of tumor cells to chemotherapeutic agents has also been confirmed,^{15–17} which suggests that miRNAs could have a broad effect on the response of cancer cells to chemotherapy.

Esophageal cancer is the eighth most common cancer and the sixth most common cause of cancer deaths worldwide.¹⁸ In spite of comprehensive available treatment, including chemotherapy, surgery and radiotherapy, the overall 5-year survival rate for patients with esophageal squamous cell carcinoma (ESCC), the most common form of esophageal cancer, remains low, at 10–40%, because of advanced disease, metastasis and resistance of the tumor to chemotherapy and radiotherapy.^{19–21} Cisplatin is the most frequently used chemotherapeutic agent for ESCC. However, given that resistance to cisplatin limits the success of treatment, elucidation of the mechanisms that regulate cisplatin resistance in ESCC is urgently needed. In the present study, we studied the biological function of miRNAs in the development of cisplatin resistance in ESCC using the KYSE series of ESCC cell lines as a model, and focused, in particular, on the regulation of apoptosis.

MATERIALS AND METHODS

Cell lines and cultures

Human KYSE cell lines that had been established from primary tumors at our institution as described previously were cultured in RPMI 1640

¹Department of Genomic Drug Discovery Science, Graduate School of Pharmaceutical Sciences, Kyoto University, Kyoto, Japan; ²Department of Nanobio Drug Discovery, Graduate School of Pharmaceutical Sciences, Kyoto University, Kyoto, Japan and ³Department of Surgery and Science, Graduate School of Medicine and Pharmaceutical Sciences for Research, Toiyama University, Toyama, Japan

Correspondence: Dr G. Tsujimoto, Department of Genomic Drug Discovery Science, Graduate School of Pharmaceutical Sciences, Kyoto University, 46-29 Yoshida-Shimoadachi-cho, Sakyo-ku, Kyoto 606-8501, Japan.

E-mail: gtsu@pharm.kyoto-u.ac.jp

Received 17 August 2010; revised 24 November 2010; accepted 26 December 2010